FAILURE PREDICTION OF ROLLING ELEMENT BEARINGS OPERATED UNDER NON-STATIONARY CONDITIONS

LEILA LUNG'ATSO MBAGAYA

MASTER OF SCIENCE
(Mechatronic Engineering)

JOMO KENYATTA UNIVERSITY OF AGRICULTURE AND TECHNOLOGY

2022

Failure Prediction of Rolling Element Bearings Operated Under Non-Stationary Conditions

Leila Lung'atso Mbagaya

A Thesis Submitted in Partial Fulfilment of the Requirements for the Degree of Master of Science in Mechatronic Engineering of the Jomo Kenyatta University of Agriculture and Technology

2022

DECLARATION

This thesis is my original work and has not been presented for a degree in any other university.

Signature..... Date...../...../.....

Leila Lung'atso Mbagaya

This thesis has been submitted for examination with our approval as university supervisors:

Signature..... Date...../...../.....

Dr.-Ing. James K. Kimotho, PhD

JKUAT, Kenya

Signature..... Date...../...../.....

Dr.-Ing. Jackson G. Njiri, PhD

JKUAT, Kenya

DEDICATION

This work is dedicated to my husband Gregory, and my sons Zac and Zayn. Thank you for believing in me.

ACKNOWLEDGMENT

First and foremost, my gratitude goes to the Almighty God for giving me the strength to pursue and complete this course successfully. Secondly, I would like to acknowledge my supervisors, Dr.-Ing. James K. Kimotho and Dr.-Ing. Jackson G. Njiri for their invaluable guidance and advice throughout my studies. Special thanks goes to Jomo Kenyatta University of Agriculture and Technology (JKUAT) for granting me the scholarship for my studies. My appreciation also goes to the staff of JKUAT for the assistance they accorded me during my studies. Special appreciation goes to my husband, Gregory, and sons Zac and Zayn, who gave me the reason to push through this journey.

TABLE OF CONTENTS

LIST OF TABLES

LIST OF FIGURES

LIST OF APPENDICES

LIST OF ABBREVIATIONS

ADT :Accelerated Degradation Testing

AI :Artificial Intelligence

ANN :Artificial Neural Network

BPFI :Ball Pass Frequency of Inner Race

BPFO :Ball Pass Frequency of Outer Race

BSF :Ball Spin Frequency

CWRU :Case Western Reserve University

CBM :Condition-Based Maintenance

CM :Condition Monitoring

DFIM :Doubly-Fed Induction Machine

DOF :Degree of freedom

DWNN :Dynamic Wavelet Neural Network

DWT :Discrete Wavelet Tranform

EMD :Emperical Mode Decomposition

EPST :Extended Phase Space Topology

FEA :Finite Element Analysis

FFT :Fast Fourier Transform

FFT :Fundamental Train Frequency

HMM :Hidden Markov Models

HMRA :High Multi-Resolution Analysis

HOES :Higher Order Energy Separation

HSMM :Hidden Semi-Markov Model

IF :Inner Race Fault

MSE :Mean Square Error

OF :Outer race Fault

PCA :Principal Component Analysis

PSO :Particle Swarm Optimisation

REB :Rolling Element Bearing

RMS :Root Mean Square

RP :Recurrence plot

RPM :Revolutions Per Minute

RQA :Reccurrence Quantification Analysis

RUL :Remaining Useful Life

SNLSE :Sequential Nonlinear Least-Square Estimation

SOAP :Spectrometric Oil Analysis Programme

STFT :Short Time Fourier Transform

TKEO :Teager-Kaiser Energy Operator

WT :Wavelet Transform

LIST OF SYMBOLS

A_1	Material property [-]
C_d	Depth of spall [mm]
D	ball diameter [mm]
L	Fatigue life [-]
Sp	Spall length [mm]
T	Contact surface dimensions [-]
W_{sp}	Spall similitude [-]
c	Clearance [mm]
c_s	Damping of shaft [Ns-m]
c_p	Damping of pedestal [Ns-m]
c_r	Damping of resonance changer [Ns-m]
dt	Time increment [s]
f_x	Ball-raceway contact force [N]
f	Ball-raceway contact force in the x-direction [N]
f_y	Ball-raceway contact force in the y-direction [N]
j	Rolling element[-]
k_b	Load deflection factor [m]
k_s	Stiffness of shaft [N-m]
k_p	Stiffness of pedestal [N-m]
k_r	Stiffness of resonance changer [N-m]
max	Maximum stress [N-m^2]
m_s	Mass of shaft [kg]
m_p	Mass of pedestal [kg]
m_r	Mass of resonance changer[kg]
n_b	Number of balls [-]

x_s	Shaft's degree of freedom in x-direction [-]
x_p	Pedestal's degree of freedom in x-direction [-]
y_s	Shaft's degree of freedom in y-direction [-]
y_p	Pedestal's degree of freedom in y-direction [-]
τ_j	Contact state [-]
τ_{avg}	Average shearing stress [N-m]
ω_c	Cage speed [rad/s]
ω_s	Shaft rotational speed[rad/s]
ω_{spin}	Ball spin frequency [rad/s]
δ_j	Overall contact deformation of the jth rolling element [m]
β_j	Fault switch [rad]
ϕ_j	Angular position of the rolling elements [rad]
ϕ_o	Previous cage position [rad]

ABSTRACT

Bearings constitute a majority of the components found in rotating machines. Though inexpensive, their failure can result in unnecessary downtime, losses in production, and propagation of failure to other critical components leading to expensive maintenance actions. Most of these rotating machinery are operated under adverse and varying conditions which result in difficulty in defining health indices from condition monitoring data. Predicting the failure of such machines is crucial to determine when the maintenance is required thereby leading to a reduction in maintenance costs and an improvement in the safety and reliability of the machines. Therefore, techniques for condition monitoring of rotating machinery operated under non-stationary conditions are necessary. This work employed a model-based condition monitoring approach to predict the failure of rotating machinery under non-stationary conditions. One of the advantages of model-based approach is the ability to incorporate physical understanding of the system monitoring. Firstly, the vibration model for rolling element bearing with fault was constructed in MATLAB/Simulink environment. An automatic parameter identification based on Particle Swarm Optimisation (PSO) algorithm was employed to identify the dynamic parameters of a rolling element bearing due to its ease of implementation and rapid convergence property. The optimized bearing parameters were then used in diagnosing bearing faults. To evaluate the feasibility of this approach, two publicly available data sets were employed. The results showed an improved average accuracy of 99.67% and 99.2% for bearing faults of Case Western Reserve University and University of Paderborn datasets, respectively. Additionally, the bearing model with estimated parameters was used to generate degradation data by varying the fault depth. Feature extraction was carried out where Root Mean Square (RMS) was determined as the appropriate health indicator. Lastly, Paris degradation model was employed to determine bearing damage and its evolution with time while factoring in speed, applied load, and bearing geometry. The remaining useful life of the bearing was found to be 1598 cycles. The prediction results and evaluation indexes demonstrated the effectiveness and superiority of the proposed method.

CHAPTER ONE

INTRODUCTION

1.1 Overview

This chapter discusses the background of condition monitoring of rolling element bearings, the problems identified in the current methods used, and the objectives that have been formulated to tackle the problem.

1.2 Condition Monitoring of Rolling Element Bearings in Rotating Machines

Rotating machineries are the most common mechanical components in industrial applications. Their main components are gear boxes, rolling element bearings, and rotary shafts. The work of bearings in rotating machines is to reduce friction and allow for smoother rotation of shafts. Typically, these machines operate under adverse conditions of high load and high temperatures. These conditions may cause severe breakdowns and decrease in the equipments performance resulting in reduced safety, availability and reliability, economic losses, and lower product quality (Jardine et al., 2006)

A good maintenance strategy is crucial in preventing catastrophic failures while maintaining machine safety and reliability as well as adding value to maintenance practices. According to Heng et al. (2009), the simplest maintenance strategy employed in the industries is known as breakdown maintenance. This is where machines are run until they fail and when failure has occurred, reactive maintenance is carried out. This approach can be extremely costly due to long hours of machine

downtime and may also lead to propagation of failure to other components. A slightly more effective time-based maintenance technique known as preventive maintenance involves periodical cleaning, servicing, and inspection of machines in order to prevent abrupt failure. However, this method cannot guarantee the absence of any breakdown and the replacement of parts before their end lifetime. In addition, there is an increase in the number of maintenance actions hence increasing the maintenance cost during the lifecycle of an equipment.

A more efficient maintenance approach is condition-based maintenance (CBM) which has been adopted to address the issue of machine reliability and reduction of maintenance related expenses. Figure 1.1 shows a schematic diagram comparing the operational, maintenance, and total cost for the different maintenance strategies. Condition-based maintenance is a maintenance strategy aimed at maximizing productivity and machine up time while lowering operating costs by carrying out maintenance when the need arises (Peng et al., 2010). The actual conditions of a machine are monitored to obtain the health status of a system and if the indicators show signs of upcoming machine failure, maintenance is carried out. A CBM program consists of two important aspects known as diagnostics and prognostics.

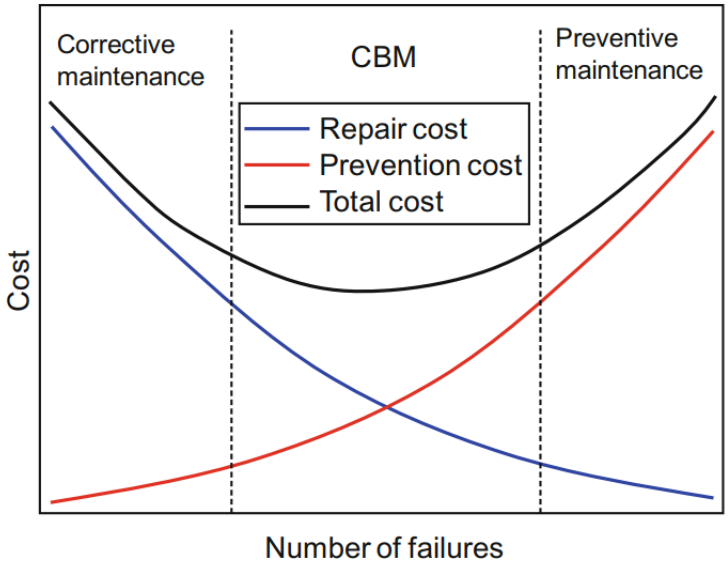

Figure 1.1: Maintenance strategies versus cost (Jardine et al., 2006)

Diagnostics is concerned with fault detection, isolation, and identification when it occurs. Fault detection indicates when a failure has occurred; fault isolation locates the faulty component; and fault identification determines the nature of the fault when it is detected. Prognostics, unlike diagnostics, is a prior event analysis process that deals with failure prediction before it occurs. It is the ability to predict accurately and within acceptable error bandwidth the remaining useful life of a failing component or subsystem. Prognostics is much more efficient than diagnostics in reducing machine downtime. Diagnostics, however, is required when fault prediction of prognostics fails and a fault occurs.

Currently, there are several methods for fault diagnosis of rolling element bearings which can be classified as data-based and model-based fault diagnosis methods. In the recent past, vibration based condition monitoring has been widely used for bearing fault detection (Zhang et al., 2007). An overview of vibration-based condition monitoring in rotating machines is given in (Sinha & Elbhbah, 2013). The wide use of such methods is because vibrational behaviour is often sensitive to small

structural variations as well as changes in process parameters. However, vibration signals are usually non-stationary in actual operation due to the changing frequencies thereby restricting the extraction effect for fault features. This affects the accuracy of fault diagnosis. Moreover, the changes in vibrational behaviour often present a confusing array of data on which to base any diagnosis and in these situations an accurate theoretical model becomes invaluable.

Model-based approach to fault diagnosis of rolling element bearings has been garnering attention in the last two decades (Mbagaya et al., 2017). This approach relies on an explicit mathematical model of the system under observation by assuming that a fault in the system will lead to deterministic changes in the model parameters. Model-based fault diagnostic approach can be more effective than other approaches that do not use models if a correct and accurate model describing the behaviour of the system is built. However, one of the biggest challenges of model-based diagnostics is accurate development of the model that captures the behaviour of the system (Gao et al., 2015).

Figure 1.2 shows the general approach of a model-based diagnostic system. Residual signals are generated using available inputs and outputs from the monitored system and they indicate the presence of a fault in the system (Isermann, 2011). The majority of the existing model-based diagnostic techniques are based on parameter estimation, parity equations or state estimation.

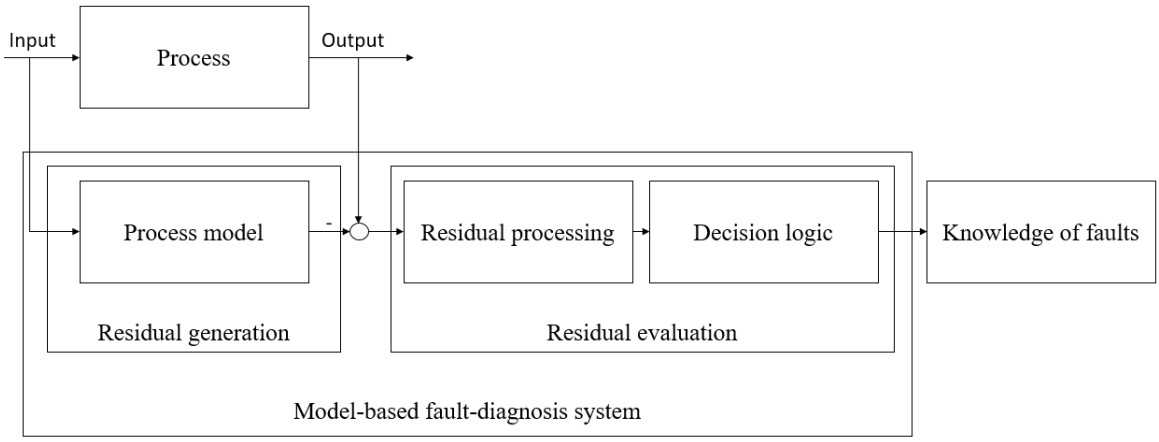

Figure 1.2: General flowchart of a model-based diagnostic system (Isermann, 2011)

Prognostics and health management (PHM) of rotating machinery, especially for bearings, has attracted extensive attention due to its effectiveness in avoiding the abrupt shutdown. One of the challenges associated with remaining useful life(RUL) estimation of bearings is building an appropriate degradation model to accurately describe the bearing degradation process. Since the objective of prognostics is to accurately predict the remaining useful life (RUL) of machinery before failure occurs, different approaches have been proposed for the RUL prediction of rolling bearings in recent decades Lee et al., 2014. These approaches can be classified into three main methods as shown in Figure 1.3. Data-driven approach relies on observable past data and statistical models(Gebraeel et al., 2004; Gebraeel & Lawley, 2008; Tobon-Mejia et al., 2010). The models are derived from routinely monitored system operating data such as oil debris, vibration signals, temperature, and pressure.

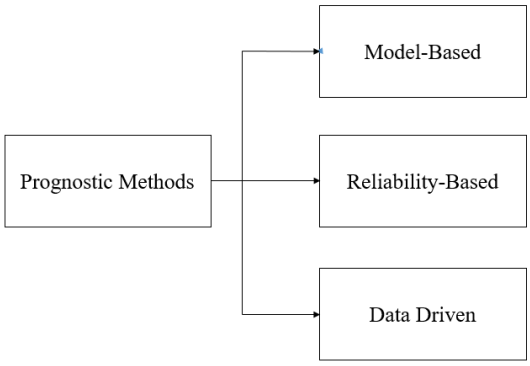

Figure 1.3: Approaches to Prognostics Gebraeel and Lawley, 2008

.

Reliability-based approaches are premised on the use of simple reliability functions such as Weibull law and exponential law, rather than complex mathematical models (Orchard & Vachtsevanos, 2009). On the other hand, model-based approaches use models derived from first principles (Kacprzynski et al., 2004; Lee et al., 2014; Li & Lee, 2005). These approaches employ residuals as features by carrying out consistency checks between sensed measurements of a system and outputs of a mathematical model.

Most of the research that has been carried out in the field of prognostics has focused on machines operating under stationary conditions. In this case, the operating conditions of a system are set at relatively constant values and condition monitoring data is acquired at suitable intervals. Rotating machines have increased complexities and complex degradation processes due to non-stationarity, which is either induced manually by the operator, or automatically through a controller or through environmental factors. Satisfactory results can therefore not be produced when traditional techniques are applied to non-stationary conditions. With increasing complex machinery, there is need for CBM techniques that are able to operate on such machines operating under non-stationary conditions such as wind turbines,

production equipment operating at intermittent conditions, and automobile drive trains.

The focus of this research is to address the challenge of coming up with a bearing model with parameters optimized to increase accuracy and that can predict the failure of rotating machines under non-stationary conditions. The key subject of this study is rolling element bearings because they have resulted in a majority of the failures in rotating machines (Bonnett & Yung, 2008) as depicted in Figure 1.4. Such an undertaking of acccurate modeling and predicting the failure of bearings can improve the safety and reliability of rotating machines while reducing maintenance costs.

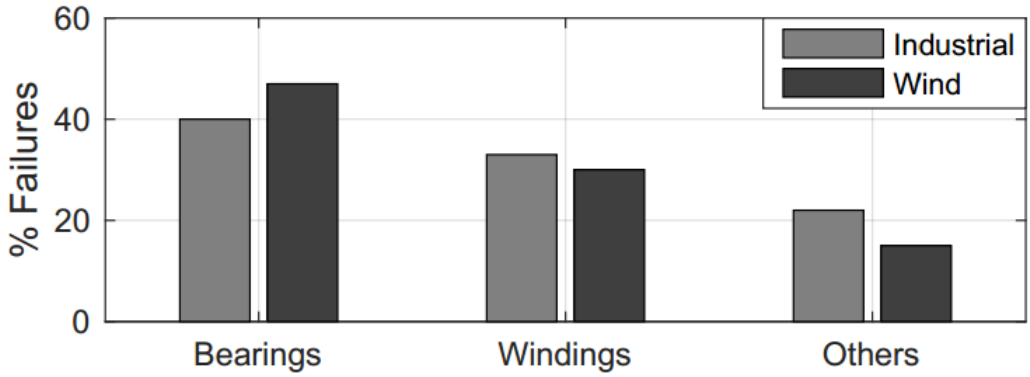

Figure 1.4: Bearing failure (Bonnett & Yung, 2008)

1.3 Problem Statement

The failure of rolling element bearings is one of the cases of breakdown in rotating machines. Statistics show that bearing failure accounts for 40% of the breakdowns that occur in rotating machinery (Djeddi et al., 2007). The failure of bearings can be catastrophic in high reliability application areas such as aerospace and automatic processing machines. Since rolling element bearings are operating in harsh conditions, their degradation in health is expected and failure of such elements can cause machine downtime and it is economically costly. It is important to have a well

developed condition monitoring (CM) program to improve the reliability of such machines.

Current trends in research on rotating machines has been limited to stationary operating conditions. However, in most practical cases, the operating conditions of rotating machinery do not remain constant in the life of the system. For example, in wind turbines, the variations in load and wind speed make it difficult to predict the failure of wind turbines due to the stochastic nature of the operating conditions. Therefore, it is critical to predict the failure of such machines that are operated under non-stationary conditions in order to save on operation and maintenance (OM) costs and improve machine reliability.

Data-based approach has been used for bearing condition-based maintenance. However, the accuracy of such an approach is dependent on the huge training data required by machine learning algorithms. Incremental learning can be employed in situations that are not included in the database used to train models. For new systems, this data is not readily available and hence it is therefore easier to incorporate a model-based approach.

Model-based approach is more effective than other approaches that do not use models if a correct and accurate model describing the behaviour of the sytem is built. However, one of the biggest challenges of model-based systems is development of the model to accurately capture the behaviour of the system. In the case of rolling element bearing, the ability to optimise the bearing parameters such as stiffness and damping will determine the accuracy of the model. With automatic parameter identification, one just needs the base model and it can be used with different sizes and geometry of similar components. Moreover, the time taken to construct a model is reduced.

1.4 Objectives

The main objective of this study is to predict the failure of rotating machinery operated under non-stationary conditions using model-based approach. To realize this objective, the following specific objectives were carried out.

1. Development of fault models and fault evolution models for rolling element bearings to be used in failure prediction
2. Automatic parameter estimation of bearing parameters using Particle Swarm Optimisation (PSO) algorithm
3. Validation of the fault models with experimental data from a dedicated test-rig for ball bearings
4. Estimation of the remaining useful life (RUL) of bearing

1.5 Justification

Failure in rotating machines is very costly in modern industries that are focused on performance and productivity. Succesful implementation of failure prediction method will result in significant cost savings and increased revenues. This will be achieved by eliminating unnecessary and costly preventive maintenance, optimizing maintenance scheduling, and reduction of the lead time for procuring the spare parts (Lee et al., 2014). This research will be beneficial to manufacturing environments, aerospace, and military applications where there is increased use of autonomous and self-optimizing mechatronic systems.

This thesis covers dynamic modelling, automatic parameter estimation, fault diagnostics, and RUL estimation of rolling element bearings operating under non-stationary conditions. The dynamic model aims to give the insights and

knowledge for further enhancements of current monitoring practices. The scope of the model is limited to diagnosing localised faults in rolling element bearings. The parameters of the bearing model are estimated using Particle Swarm Optimisation algorithm. Estimation of the Remaining Useful Life (RUL) of the bearing was carried out using Root Mean Square (RMS) as the primary health indicator.

1.6 Organisation of the Thesis

This thesis is composed of five themed chapters:

Chapter 1 is the introductory chapter. Here, the relevant background information on rolling element bearing failure in rotating machines is given. The problem statement, objectives of the research and justification are also presented in this chapter.

Chapter 2 provides the literature review on fundamentals of rolling element bearings, parameter estimation of bearings, bearing diagnostics and prognostics. In addition, the identified research gaps have been stated in this chapter.

Chapter 3 is the methodology chapter. It highlights the development of the bearing model, the identification of bearing dynamic parameters using Particle Swarm Optimisation algorithm , diagnosis of bearing faults and remaining useful life estimation procedure using Root Mean Square (RMS) as the health indicator.

Chapter 4 provides the results and discussion from bearing development, bearing parameters estimation using Particle Swarm Optimisation (PSO) algorithm, the simulation of the bearing degradation process, feature extraction, development of degradation model using Paris law, and remaining useful life estimation. Results from validation of the models using two publicly available datasets is also discussed.

Chapter 5 is the conclusion and recommendations chapter. Here, the findings of this research work are provided and recommendations for future research have been provided.

CHAPTER TWO

LITERATURE REVIEW

2.1 Introduction

This chapter looks into the major concepts of rolling element bearing failure, approaches of bearing diagnostics and prognostics, parameter estimation techniques in bearing diagnostics, and bearing prognostics. The chapter also reviews previous work done by other researchers and identifies gaps from these researches.

2.2 Rolling Element Bearings

Rolling element bearings are mechanical elements that are used when rotating or linear motion between two moving parts is required. They consist of four components: the inner race, outer race, cage, and rolling components as shown in Figure 2.1.

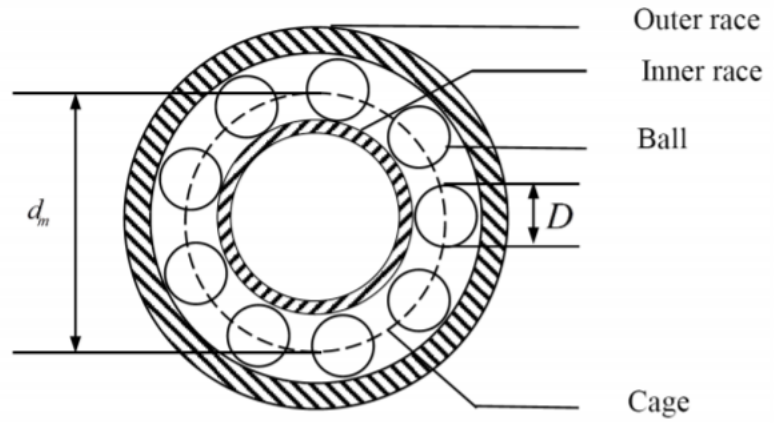

Figure 2.1: Rolling element bearing components (Liu et al., 2013)

2.2.1 Rolling Element Bearing Failure

Statistics show that bearing failure is one of the main causes of breakdown in rotating machinery (Alewine & Chen, 2012). Failure of rolling element bearings may occur in different ways and at different stages of their service life. Some of the bearing failures that may occur during the early stages of their service life may be due to inappropriate design, faulty installation, brinelling or overload. When a bearing nears the end of its lifetime, failure may be caused by fatigue, contamination, lubrication, fracture or creep.

In cases where the bearing is well aligned, properly loaded and sufficiently lubricated, the failure that occurs is caused by rolling element contact fatigue. This failure is due to application of repeated stresses on a finite volume of material (Roemer et al., 2008). The result is that material from the load bearing surface of rolling elements and raceway flakes off leaving a spall or a pit as shown in Figure 2.2.

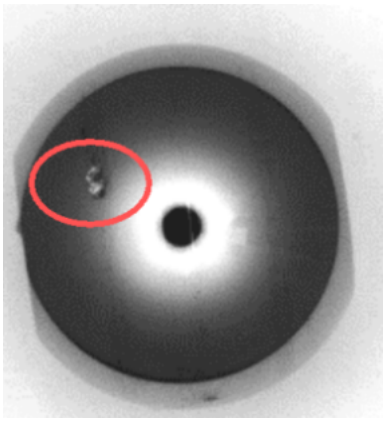

Figure 2.2: Ball bearing with a spall (Roemer et al., 2008)

Once a spall is initiated, it quickly grows and develops and the appearance of a spall is usually a sign of bearing failure. However, in some applications, there is usually a lapse of time from initiation of first spall to the end of the useful life of a bearing. A study by Harris (2001) showed that 3 to 20 % of a particular bearings useful life remains after spall initiation.

2.2.2 Bearing Characteristic Faults

When a single point defect occurs in any part of the bearing, a high frequency resonance is excited in the structure of the bearing as the defect comes into contact with the elements in the bearing. This frequency is known as characteristic frequency and it can indicate the type of fault present in a bearing (Sawalhi & Randall, 2008). The most common rolling element bearing faults are damage of the inner race, outer race, cage fault, and rolling element fault (Sawalhi, 2007). The inner race damage, Ball Pass Frequency of Inner Race (BPFI), is expressed as

$$BPFI = \frac{n_b f_r}{2}\left(1 + \frac{D_b}{D_p}\cos\alpha\right). \tag{2.1}$$

Outer race fault also known as Ball Pass Frequency of Outer Race (BPFO), is given by

$$BPFO = \frac{n_b f_r}{2}\left(1 - \frac{D_b}{D_p}\cos\alpha\right). \tag{2.2}$$

Cage fault also known as Fundamental Train Frequency (FTF) is given by

$$FTF = \frac{f_r D_b}{2D_p}\left(1 - \frac{D_b}{D_p}\right)\cos\alpha. \tag{2.3}$$

The rolling element fault also known as Ball Spin Frequency (BSF) is expressed as

$$BSF = \frac{n_b f_r}{2}\left(1 - \frac{D_b}{D_p}\cos\alpha\right). \tag{2.4}$$

Here, n_b is the number of rolling elements, D_b and D_p are the rolling element diameter and the pitch diameter of the bearing respectively, f_r is the rotational speed of the inner race (shaft speed) and α is the radial contact angle (Sawalhi, 2007).

2.2.3 Fatigue Spall Initiation and Propagation

2.2.3.1 Spall Initiation

Many modern theories that exist for predicting spall initiation from bearing dimensions are based on Lundberg-Palmgren (L-P) Model (Harris & Yu, 1999). Yu and Harris (2001) proposed a new stress-based fatigue life model where the empirical data required to complete the model can be obtained using element testing in lieu of complete bearing testing employed by L-P.

According to Yu and Harris (2001), the typical equation that is used to predict the life of a bearing is a function of the basic dynamic capacity Q_c and the applied load as stated below

$$L_{10} = \left(\frac{Q_c}{Q}\right)^{\frac{(z+x+y)}{3}} \tag{2.5}$$

where L_{10} is the life of a bearing, Q is an applied load, and Q_c is dynamic capacity. Here,

$$Q_c = A_1 D^{\frac{(2z-x-y)}{(z+x+y)}} \left[\left(\frac{T}{T_1}\right)^z \frac{u(D\Sigma\rho)^{\frac{(2z-x-y)}{3}}}{(a^*)^{z-x}(b^*)^{z-y}} \frac{d}{D}\right]^{\frac{-3}{z+x+y}} \tag{2.6}$$

where A_1 is material property, T is a function of contact surface dimensions, T_1 is value of T when $a = b = 1$, u is number of stress cycles per revolution, D is ball diameter, ρ is curvature (inverse radii of component), d is component (raceway) diameter, a is function of contact ellipse dimensions, b is function of contact ellipse dimensions and x, y, z are the axes.

2.2.3.2 Spall Propagation

Once a fatigue spall has been generated, vibratory loads, heat generation rates and contact stresses increase. This results in formation of more fatigue cracks within the subsurface of the bearing. Raje et al. (2008) propagated rolling element bearing

fatigue spalls well beyond the laboratory criteria of 6.5 mm^2. His experiments indicated that the propagation of rolling contact fatigue beyond its initial appearance is a highly variable process.

Li and Lee (2005) predicted spall progression of tapered roller bearings using an empirical method. The empirical constants need to be determined for all bearings and all operating conditions for which is used. Harris (2001) presented a spall progression model by extending the I-H fatigue life theory. With their model, prediction of the life of a spall progression was achieved so long as bearing fracture does not occur. The equations relating spall progression rate $\frac{dSp}{dN}$ to spall length Sp are as follows;

$$\frac{dSp}{dN} = C((\theta_{max} + \tau_{avg})\sqrt{\pi Sp})^m \tag{2.7}$$

where θ_{max} is maximum stress, τ_{avg} is average shearing stress, Sp is spall length, C and m are constants.

The research done by Harris (2001) showed that 3 to 20% of a particular bearings useful life remains after spall initiation. The study identified two spall progression regions as shown in Figure 2.3. Stable spall progression region characterized by gradual spall growth and minimum vibratory loading and unstable spall region characterized by increasing broadband vibration amplitudes.

Orsagh et al. (2003) used the progression model of Kotzalas and Harris and compared the predicted progression size with oil particle quantity. The findings revealed a correlation between the oil debris data and the spall size. Scaling of the oil particle quantity was then done to approximate spall size. For an ideal result to be obtained, various physics parameters of this model such as material constants should be determined accurately by numerical experiments.

Roemer et al. (2008) implemented bearing prognosis in three modules as shown in Figure 2.4. The first module is diagnostic where variables for bearing diagnoses

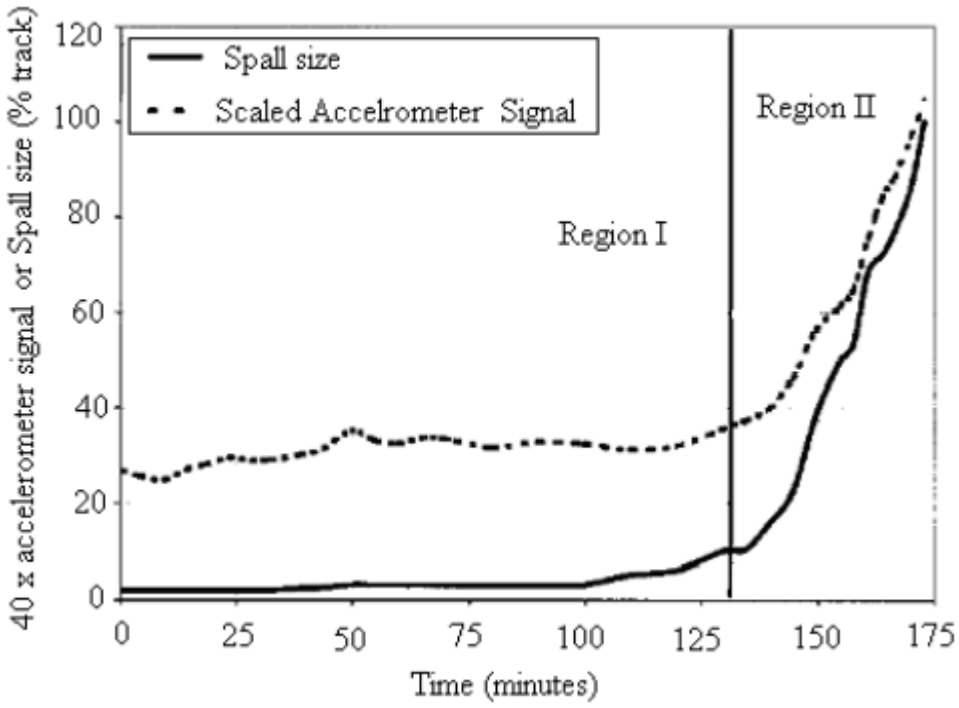

Figure 2.3: Scaled accelerometer signal and spall size as a function of time Harris, 2001

are measured. Such variables include vibration, acoustic emissions and oil debris data. Second module is where health assessment of current bearing is done with input from the diagnostic features. Prognostic Module then takes over where failure prediction is done based on presence of the incipient fault. The drawback of this approach is model uncertainties and development of the fault earlier than predicted or without warning.

2.2.4 Modelling the Vibration of Localized Defects

Diagnostics and prognostics benefit highly from the ability to model the vibration of localized defects. This is due to the signals that are produced with well-defined characteristics rather than randomly waiting for the signals to show up. Simulation

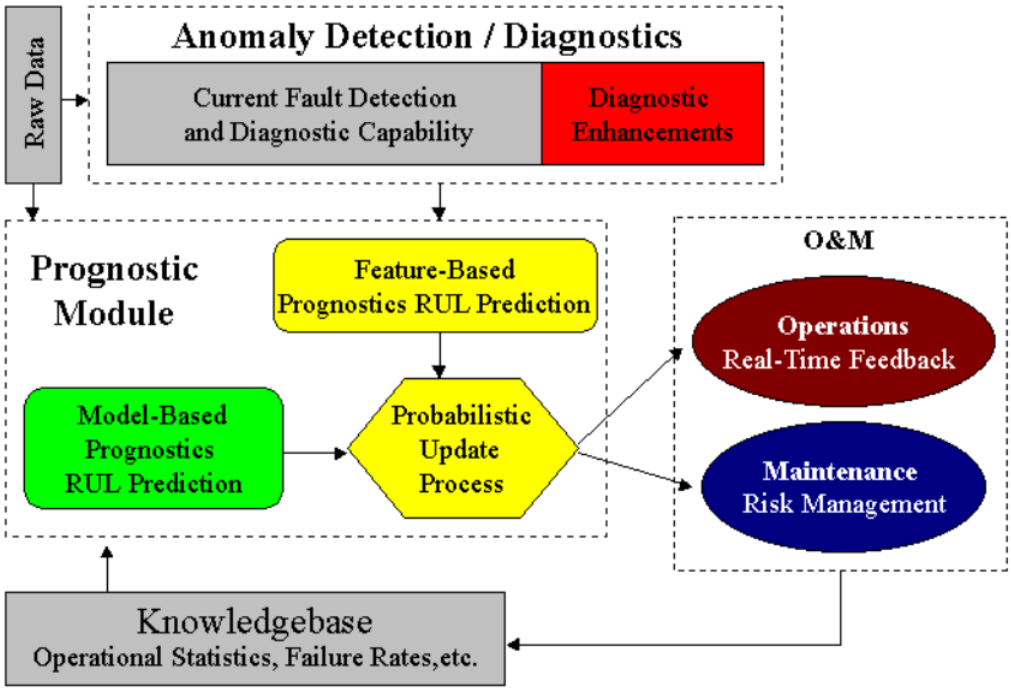

Figure 2.4: Prognostic bearing model approach (Roemer et al., 2008)

is also valuable for giving a better understanding of how faults are generated, in particular where non-linear interactions are involved. Bearing fault simulations can also be used to evaluate the effectiveness of different bearing diagnostic techniques and their performance under the influence of noise masking (Sawalhi, 2007). The main techniques to diagnose and examine rolling element bearings defects using vibration analysis are time domain, frequency domain, time-frequency domain and envelope analysis Jardine et al., 2006.

2.3 Diagnostics

There are several methods for fault diagnosis of rolling element bearings which can be classified as data-based and model-based fault diagnosis methods. In the recent past, vibration based condition monitoring has been widely used for bearing fault detection (Zhang et al., 2015). An overview of vibration-based condition monitoring in rotating

machines is given in (Sinha & Elbhbah, 2013). The wide use of such methods is because vibrational behaviour is often sensitive to small structural variations as well as changes in process parameters. However, vibration signals are usually nonstationary in actual operation thereby restricting the extraction effect for fault features. This affects the accuracy of fault diagnosis. Moreover, these changes in vibrational behaviour often present a confusing array of data on which to base any diagnosis and in these situations an accurate theoretical model becomes invaluable.

This thesis focuses on model-based approach to fault diagnosis of rolling element bearings since it has been garnering attention in the last two decades (Mbagaya et al., 2017). This approach relies on an explicit mathematical model of the system under observation by assuming that a fault in the system will lead to deterministic changes in the model parameters. Model-based fault diagnostic approach can be more effective than other approaches that do not use models if a correct and accurate model describing the behaviour of the sytem is built (Jardine et al., 2006). However, one of the biggest challenges of model-based diagnostics is development of the model that accurately captures the behaviour of the system (Gao et al., 2015). In the case of rolling element bearing, the ability to accurately describe the bearing parameters such as stiffness and damping will determine the accuracy of the model and thus, the accuracy of fault diagnosis (Sawalhi, 2007).

2.4 Parameter Estimation Techniques in Bearing Diagnostics

Parameter estimation has been a focus in recent decades with several applications to estimation of the dynamic parameters of bearings Tiwari et al., 2004. Parameter estimation relies on the principle of comparing the parameters of a defective system with the parameters of a healthy system. Therefore, a theoretical dynamic model of the process is important to apply parameter estimation methods (Isermann, 2011).

Some authors have attempted to estimate the bearing dynamic parameters using experimental techniques such as random, impulse, and unbalance excitation techniques. Tiwari and Chakravarthy (2006) presented an algorithm for identification of bearing dynamic parameters and residual unbalances, by using impulse response measurements. Another research done by Jiang et al. (2015) developed a multi-degree of freedom rotor model to identify the effective stiffness and damping of an active magnetic bearing system. However, both these method were time-consuming, not robust to noise and required the bearings to be tested in isolation thus affecting the accuracy of the obtained parameters.

Sudhakar and Sekhar (2011) employed two different approaches for the identification of unbalance fault in a rotor system. One of the methods was equivalent loads minimization while the other was vibration minimization method. The study showed that vibration minimization method identified unbalance fault with less error when compared with equivalent loads minimization method where the modified theoretical fault model is used. Regardless of this, the accuracy of the model is not guaranteed due to the 2% error that was encountered.

Samadani et al. (2014) presented an application of recurrence plots (RPs) and recurrence quantification analysis (RQA) for parameter estimation-based diagnostics of nonlinear systems. To demonstrate the procedure, a detailed nonlinear mathematical model of a servo electro-hydraulic system was used. This approach was time consuming and computationally demanding, thus makes it hard for it to be applied in an automated manner or for it to be integrated into a control system. An improvement of this approach was done by Mohamad et al. (2018) who employed an Extended Phase Space Topology (EPST) method for model-based fault detection and diagnostics of an electrohydraulic system. The drawback of this aproach was that the proposed method was only applied to numerical data obtained from the mathematical model of the system and the accuracy of the model was not guaranteed since no validation of the results with experimental data was done.

Several authors have employed algorithms with respect to parameter estimation of bearings. The most common algorithm that has been employed is the least squares method. Alonge et al. (2001) applied least squares techniques techniques together with genetic algorithm (GA) in parameter identification of induction motors. The least squares method required lower computation time than that based on GA, but it was not accurate in estimation of parameters.

Another author, Kim et al. (2007) used a hybrid evolutionary algorithm as an optimization tool in bearing parameter identification. The methodology was based on global optimization scheme using measured unbalance response of rotorbearing system. Results showed that the proposed methodology was effective in identification of bearing coefficients and the magnitude of unbalance using the measured unbalance response. However, there is need for further investigations in order to increase the accuracy and reliability of the identified results.

Tiwari and Chougale (2014) presented an identification algorithm for the estimation of dynamic parameters of Active Magnetic Bearings (AMBs) and rotor residual unbalances. The proposed algorithm was applied to experimental data from a test rig. The results showed that the algorithm was able to detect the AMB dynamic parameters, However, some inconsistencies were noted due to variations of the estimated parameters from the theoretical ones.

Mao et al. (2016) employed a transfer matrix method and a computational to identify the bearing dynamic parameters of a flexible rotor-bearing system. The proposed method was tested with a numerical example and experimental application. The results showed that it is robust to the noise and is computationally less expensive. However, it was only applied to one set of bearing size and geometry.

Han et al. (2013) presented a method based on Kriging surrogate model and evolutionary algorithm to identify the bearing parameters and unbalance information

in rotor-bearing system. The developed algorithm was tested with numerical example and experimental application. The method was more robust to noise compared to other traditional identification techniques and it is less computationally expensive. However, some modeling errors still exist due to the lack of precision in bearing parameters with some sample sizes. This inaccuracy of the model leads to a search for a method that will still reduce computational time while maintaining the accuracy required in modelling.

Recently, Particle Swarm Optimisation (PSO) algorithm has gained much attention with wide application in different fields due to its simple concept, easy implementation, and fast convergence. Particle Swarm Optimisation is a population-based evolutionary algorithm that provides an efficient means of estimating the bearing parameters and was discovered by Kennedy and Eberhart in 1995 Eberhart and Kennedy, 1995. The algorithm is based on the simulation of predation by birds and swarm intelligence.

The few simple lines required to describe the basic algorithm and the derivative free search for the solution make PSO an easy-to-use algorithm for real life problems. Like well known stochastic optimization methods such as Evolutionary Strategies or Simulated Annealing, PSO is not restricted to a local solution of the optimization problem. Thus, the solution does hardly depend on an initial starting point which can be of great advantage in the optimization process searching for novel designs.

Deng et al. (2019) employed empirical mode decomposition, fuzzy information entropy, improved PSO algorithm and least squares support vector machine (LS-SVM) in order to effectively diagnose the fault of motor bearing. The empirical mode decomposition and fuzzy information entropy were used to effectively extract the fault features, and the improved PSO algorithm was used to optimize the parameters of the LS-SVM. There was improved classification accuracy with PSO. Xia et al. (2016) employed a key kernels-PSO (KK-PSO) method for the fault

diagnosis of rotor-bearing system. The analysis results indicated that the irritating infinite-solution problems in the traditional identification methods can be resolved effectively by the KK-PSO method. Therefore, the simplicity in computation and rapid convergence property has made PSO useful in parameter identification of bearing systems (Feng et al., 2013).

Figure 2.5 presents a block diagram showing the principle of PSO-based parameter estimation. The initial state X_o is given to both the real system X and the estimated model $\hat{X}$. Then outputs from the real system and its estimated model are input to the optimization algorithm, where the objective function is calculated (Alfi, 2011). Since this algorithm depends on the objective function to guide the search, it must be defined before initialization is carried out. The fitness function of estimated model parameters is considered to be the mean squared error (MSE) between real and estimated responses for a number of given samples. Hence, the objective function is given as

$$MSE = \frac{1}{N}\sum_{k=1}^{N}\left[X(k) - \hat{X}(k)\right]^2 \tag{2.8}$$

where N is the sampling number, $X(k)$ and $\hat{X}(k)$ are real and estimated values of state vector at time k, respectively.

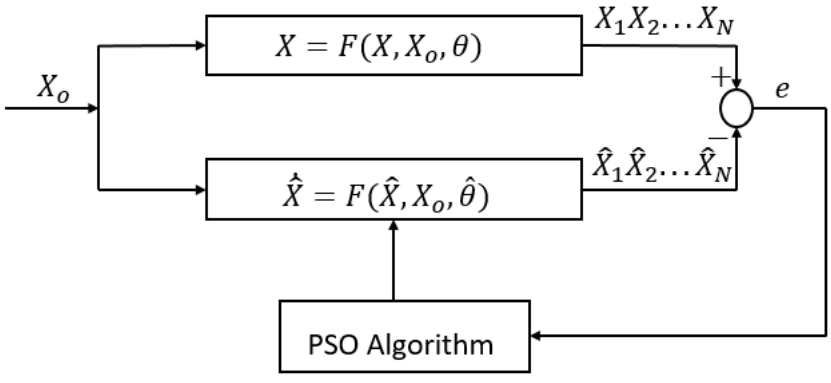

Figure 2.5: Principle of parameter estimation (Alfi, 2011)

With automatic parameter identification using PSO, one just needs the base model and it can be used with different sizes and geometry of similar components. Moreover, automatic parameter identification reduces the time taken to construct a model. When compared to algorithms such as GA, more research is being carried out using PSO algorithm in parameter estimation of nonlinear dynamic systems due to its simple concept, easy implementation, and fast convergence (Shi et al., 2001). The simplicity in computation and rapid convergence property has made it very useful in parameter identification of this system as it will be seen in the subsequent sections. Moreover, fewer parameters are needed in PSO.

2.5 Prognostics

The field of prognostics has encountered several advancements in the past 10 years (Lee et al., 2014). Various techniques that have been successfully employed for prognostics include vibration analysis, oil analysis, temperature analysis and acoustic emissions. These methods are effective in describing machine performance. The two main categories used to describe the different approaches to prognosis are data-driven approaches and model-based approaches. In this section, studies that are related to prognostics under non-stationary conditions are reviewed.

2.5.1 Data-driven-Approach to Prognostics

Data-driven methods are based upon statistical and learning techniques and are derived from routinely monitored system operating data such as oil debris, vibration signals, temperature, and pressure. Most of the data-driven approaches originated from the theory of pattern . They mainly comprise of Artificial intelligence (AI) techniques and statistical methods (Jardine et al., 2006). Statistical methods include state space models (e.g Bayesian networks (Elwany & Gebraeel, 2008), hidden Markov Models (HMM) and hidden semi-Markov Models (HSMM) (Dong & He, 2007)) and regressive models while AI techniques include neural networks (Malhi

et al., 2011).

Figure 2.6 illustrates the stages in a data-driven approach. Data acquisition involves measuring the appropriate form of data. The measured condition monitoring data can be vibration data, acoustic data, oil analysis data, etc. The data measured is polluted by different types of noise. Pre-processing removes the noise through filtering and prepares it for feature extraction. Feature extraction involves processing the filtered data. It can be performed in the time-domain, frequency-domain or time-frequency domain. After this has been done, post-processing is then carried out to prepare feature vectors for pattern recognition stage. Pattern recognition is where a method is applied to decide the damage state based on the feature vectors extracted by signal processing techniques (Peng et al., 2010).

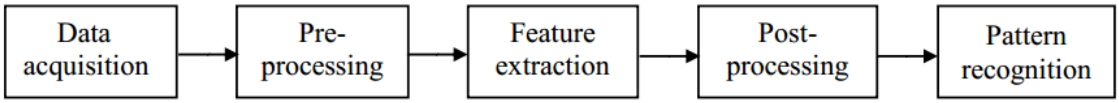

Figure 2.6: Data-driven prognostic approach (Peng et al., 2010)

Data-driven approach is advantageous over model-based approach in cases where the system is complex and thus accurate modeling becomes expensive. Moreover, data-driven approach is applicable where an understanding of first principles of system operation is not comprehensive. However, the primary drawback of such approach is that effectiveness is not only dependent on the quantity but also quality of system operational data. The systems require large amount of training data and it may have wider confidence intervals in comparison to other approaches. Furthermore, it is difficult to obtain run-to-failure data particularly for new systems because running systems to failure could be lengthy and costly.

Gebraeel et al. (2004) predicted bearing failure time by using the artificial neural network (ANN) approach. An experimental setup was developed to perform

accelerated bearing tests where vibration information was collected from a number of bearings that are run until failure. This information was then used to train neural network models on predicting bearing operating times. Vibration data from a set of validation bearings were then applied to these network models. The resulting predictions were used to estimate the bearing failure time. Comparisons between these predictions with the actual lives of the validation bearings and errors were computed to evaluate the effectiveness of each model. The results showed that 64% of the predictions were within 10% of actual bearing life, while 92% of predictions were within 20% of the actual life. However, the drawback of this method is that the failure thresholds were not adequately defined.

A trained dynamic wavelet neural network (DWNN) was employed by vachtsevanos2001fault in prognosis of a defective bearing with a crack in its inner race. It was noted that more extensive failure data, that is difficult to obtain in critical processes, is required to draw firm and comparative conclusions.

A Recursive bayesian technique was proposed by Zhang et al. (2007) to estimate asset health reliability using condition monitoring data. This method enabled reliability evaluation using observations from individual assets, rather than using failure data from a population of assets. Validation of the employed method was implemented by an experiment on bearing life testing as a case study. The accuracy of such a technique relies strongly on the correct determination of thresholds for various trending features (Lee et al., 2014).

Hidden Markov models (HMMs) were integrated with an adaptive stochastic fault prediction model and principal component analysis (PCA) and used in bearing prognosis by Zhang et al. (2005). The principal features extracted by PCA were utilized by HMM to generate a health/degradation index representing the current system health status. This was then used as an input to an adaptive prognostics component for on-line remaining useful life prediction. The merit of this approach is

the on-line learning capability which increases its prediction accuracy. However, the inability to physically observe a defect n an operating unit makes it difficult to relate the defined health-state change point to the actual defect progression. Chinnam and Baruah (2003) also employed HMMs to model degradations on bearings, and to estimate the underlying RUL.

Dong and He (2007) presented a statistical modelling methodology based on segmental hidden semi-Markov models (HSMMs). An HSMM is a hidden Markov model (HMM) with temporal structures. However, unlike HMMs, HSMMs employ explicit probability distributions such as Gaussian distribution to model the state durations more accurately. The developed method was then tested using data from a real hydraulic pump health montoring application case study. The results showed that the recognition rates for all states were greater than 96%. For each individual pump, the recognition rate increased by 29.3% in comparison with HMMs. However, the limitation experienced is the difficulty in relating the defined health-state change point to the actual defect progression since it is often impractical to physically observe a defect in an operating unit.

2.5.2 Model-based Approach to Prognostics

The model-based prognosis approach relies on a mathematical model of system under observation by assuming that a fault in the system will lead to deterministic changes in the model parameters. Input includes information on operating and environmental conditions. A comparison of model output to actual system outputs is done to generate a residual signal as depicted in Figure 2.7. The ratio of output and input can be used as a health index to track degradation of the system (Daigle & Goebel, 2011). Based on that generated signal, useful information is extracted and potential fault conditions are identified.

A common model-based approach is crack growth modelling. Li and Lee (2005)

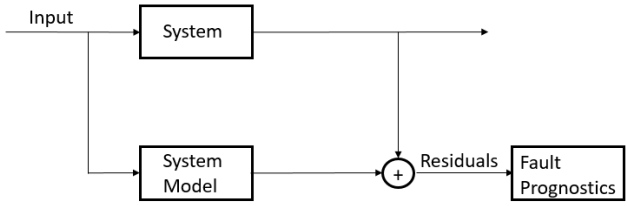

Figure 2.7: Model-based prognostic approach (Daigle & Goebel, 2011)

based their bearing prognostic methodology on the in process adaptation of defect propagation rate with vibration signal analysis. The defect size as predicted by a fatigue crack propagation model was compared to the estimation from a diagnostic model in the future to fine tune the propagation model parameters. However, the assumption that the defect size can directly be estimated from vibrations is faulty since the instantaneous defect size cannot be measured without interrupting machine operation.

Lee et al. (2014) used an embedded gear dynamic model to predict the remaining useful life (RUL). The advantage of this model is that finite element analysis (FEA) enables stress calculation based on the gear geometry, speed, load, material properties and so on. However, this method is time consuming, needs expensive software to analyze the vibration data and calculate the stress value, and the results rely on the accuracy of the defect size.

Oppenheimer and Loparo (2002) used Forman Law of linear elastic fracture mechanics to model rotor shaft crack growth. The assumption made from these crack growth models is that the defect size could be estimated directly from vibration data. This assumption, however, is questionable since instantaneous defect size cannot be measured without interrupting the operation of the machine thereby hindering the usefulness of this model.

Bian and Gebraeel (2014) investigated a method for modeling degradation signals

from components functioning under dynamically-evolving environment conditions. In-situ sensor signals were utilized in real time to predict and update the distribution of a components residual lifetime. The research showed that the Bayesian updating scheme provides reasonable lifetime prediction results, especially as information is progressively revealed over time. However, this is based on the simplified assumption that the current environmental or operational conditions affect the time-dependent rate at which a components degradation signal increases.

Gašperin et al. (2011) modelled feature time series as an output of dynamic state model. The model was then used to determine the presence of a fault and predict the future behavior and remaining useful life of a system. The optimal model at the current state of failure is found by adopting an algorithm for on-line model estimation. The approach is validated using the experimental data on a single stage gearbox. The results showed that the model can be used to predict the evolution of the fault under variable operating conditions, if the future time profile of the load is known. Moreover, a linear relationship was assumed between operating conditions, fault dimension and vibration feature value.

The research done by Liao and Tian (2013) was also based on simplified assumptions on the relationship between operating conditions and the rate of degradation. An enhanced Bayesian technique for predicting the RUL of a single unit under time-varying operating conditions was investigated. The approach integrates in situ degradation measurements of the interested unit as well as the operating conditions with a population-based Accelerated Degradation Testing (ADT) model. The results showed that the proposed approach is capable of achieving accurate RUL prediction under complex operating conditions that may involve stochastic components. However, more test units need to be considered and further investigation into the different failure modes needs to be done.

Zhang et al. (2005) developed an integrated prognostics approach to deal with

time-varying operating condition, which integrates physical gear models and sensor data. The degradation model is built on the physics of damage progression, which takes the form of a function of environmental parameters. Any changes of these environmental parameters, such as load, temperature, and speed can be manifested immediately in the physical model. The assumption that future loading conditions are known may lead to difficulty in quantifying the remaining useful life. Moreover, validation of the proposed model with experimental investigations in a lab environment did not take place. Therefore this model may not represent the physical behavior of the target system.

2.5.3 Prognostic Techniques

The various techniques that have been successfully employed for prognostics include vibration analysis, oil analysis, temperature analysis, acoustic emissions and so on. Vibration analysis has been used to predict the RUL of bearing by use of current and previous vibration data and for diagnosis of all types of fault, either localized or distributed.

Vibration-based signal analysis can be performed in the time domain, the frequency domain or the time-frequency domain. Monitoring the variation in statistical indices such as kurtosis, root mean square (RMS) value or crest factor can help detection of bearing faults in the time-domain analysis (Hiyama et al., 2008). The disadvantage with this method is that it is difficult to determine appropriate thresholds which should not be exceeded because variations exist in different applications. Frequency-domain analysis is based on time-frequency transformation and the most popular diagnostic method uses Fourier Transform. The presence of fault characteristic frequency indicates a fault in bearing diagnosis. The main disadvantage of frequency domain analysis is inability to locate particular frequency in time domain. To overcome this problem, time-frequency analysis is used.

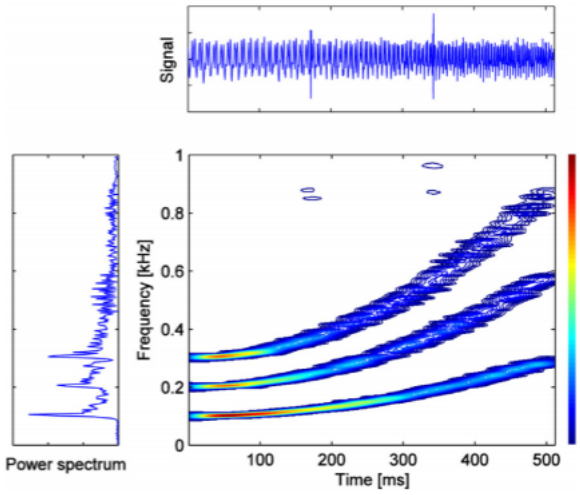

Figure 2.8: Short time fourier transform spectogram (Boashash, 2015)

Time-frequency domain techniques can be used to analyze non-stationary signals. A popular time-frequency analysis is the Short Time Fourier Transform (STFT) (Boashash, 2015) which is a Fourier-related transform that determines the sinusoidal frequency and phase content of local sections of a signal as it changes over time. Figure 2.8 shows the spectrogram obtained using STFT. The three time-varying frequency components can be observed. However, this method is limited in its time-frequency resolution. Cocconcelli et al. (2012) enhanced the fault signature of a ball bearing under varying motor-speed by averaging the short-time fourier transform (STFT) for each shaft revolution in the time-frequency domain. The sum of the averaged STFT coefficients was used as an indicator of the level of damage on the bearing. However, the relationship between the damage indicator and varying shaft speed is lacking.

Feng and Liang (2014) presented a time-frequency analysis method based on the Vold-Kalman filter and higher order energy separation (HOES) to extract fault symptoms in a wind-turbine gearbox under non-stationary conditions. The results showed that it was effective in diagnosing gear faults. However, investigation on how the faults evolve with time was not done.

An alternative to STFT is the Wavelet Transform (WT) which has more flexible time-frequency resolution and is more applicable in fault detection. This method can be classified according to signal decomposition paradigms as continuous WT, discrete WT and wave packet analysis. Pathak (2009) proposed the use of discrete wavelet transform (DWT) with high multiresolution analysis (HMRA) of stator currents for fault diagnosis of rotors in doubly fed induction machine (DFIM). However, this approach was only evaluated for fault diagnosis.

Guan et al. (2017) presented a time-frequency method that outperforms others in providing fine-resolution timefrequency preparation. The synchrosqueezing transform-based method was effective in detecting distributed and localized gear faults under nonstationary conditions. However, the method was not evaluated on ability to track evolution of the faults.

Antoniadou et al. (2015) presented a time-frequency analysis approach for condition monitoring of wind turbine gearboxes under varying operating condition. The Empirical Mode Decomposition (EMD) method was used to decompose the vibration signals into meaningful signal components associated with specific frequency bands of the original signal. Furthermore, the Teager-Kaiser energy operator (TKEO) approach was employed to improve the estimation of instantaneous spectral characteristics of the vibration data under certain conditions. In this approach, the relationship between the operating conditions and the features is assumed.

Wang and Zhang (2005) predicted the residual life of aircraft engines monitored based upon available oil monitoring information. The fundamental concept behind the model is the proportional residual life that assumes the residual life is proportional to the actual wear measured by the oil analysis programmes. The oil analysis data used was the total metal concentration obtained using Spectrometric Oil Analysis Programme (SOAP) from aircraft engines. The principal component analysis PCA was applied to preanalyze the data. The goodness-of-fit test was then carried out to

test the model established. The results obtained from the analysis showed that it is feasible to model the relationship between residual life and information obtained from an oil analysis program. However, this model required the determination of a threshold level to indicate defect initiation point, which is in practice, difficult to determine.

Orchard and Vachtsevanos (2009) employed particle filtering for prognosis in turbo engine. Particle filtering was used in the proposed method as CM data to monitor turbine blade health. The particle filtering algorithm consecutively updated the current state estimate for a nonlinear state-space model (with unknown time-varying parameters), and predicted the evolution in time of the probability distribution for the crack length. Authors reported acceptable results in terms of precision and accuracy. However, this method registers poor performance with high dimensional data.

2.6 Summary of Identified Research Gaps

A lot of research is currently being conducted on diagnostics and prognostics of rotating machines with the aim of improving reliability, reducing life-cycle costs and increasing the machines safety and availability. While there are so many benefits in this field, many industries have not adopted the approaches listed in this literature. The identified research gaps are as follows:

1. Most of the research done does not depict how the faults evolve with time and failure thresholds under non-stationary conditions are not defined. Most of the literature available focuses on stationary operating conditions which is not the case for many practical cases where the operating conditions vary during the lifetime of the system. In this case, it is challenging to define health indices and to define failure thresholds.

2. Another major challenge that has been highlighted in literature is to develop methods that are capable of handling real-world uncertainties that lead to accurate predictions. Some uncertainties are caused by model simplification and model parameters. Some of the research work featured employ simplified assumptions on the relation between operating conditions and the rate of degradation. The accuracy of the model is crucial in model-based condition monitoring. Parameter estimation then is the most important step in model-based diagnostics and prognostics because once model parameters are determined, accuracy of the model is guaranteed and predicting the remaining useful life is straightforward.

3. Moreover, research works with proposed models have not been validated with experimental investigations and as such may not represent the physical behavior of the target systems. It is therefore evident that methods for prognostics of systems under stochastic non-stationary operating conditions need to be investigated.

CHAPTER THREE

METHODOLOGY

3.1 Overview

The purpose of this chapter was to emphasize the model-based diagnostics and prognostic components that were used to realize the objectives. Diagnostics included the creation of a bearing model, the identification of bearing dynamic parameters using the Particle Swarm Optimisation (PSO) technique, as well as simulation and diagnosis of bearing defects. The first step in prognostics was to simulate the bearing degradation process in order to generate vibration data. After that, feature extraction was performed, and a good health indicator was chosen. Finally, estimation of the Remaining Useful Life (RUL) wasdescribed.

3.2 Diagnostics

Figure 3.1 is a block diagram summarizing the model-based diagnostic approach that was employed. The process began with a development of the bearing model in SIMULINK environment. The parameters of the model were then optimized using PSO algorithm. The model with estimated parameters was then used to carry out bearing fault diagnostics.

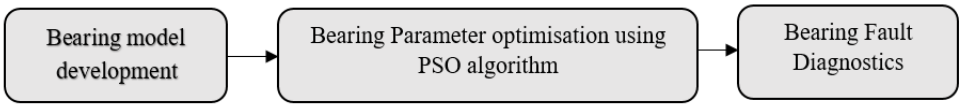

Figure 3.1: Block diagram showing the Model-Based Diagnostic Approach

3.2.1 Modelling of a Rolling Element Bearing

A simple rolling element bearing was modeled as a lumped mass-spring-damper system. The model proposed by Sawalhi and Randall (2008) was adopted in this study. The model has five degrees of freedom (DOF) as shown in Figure 3.2. A slight modification was made to introduce damping in the shaft/inner race which had not been done in the initial model.

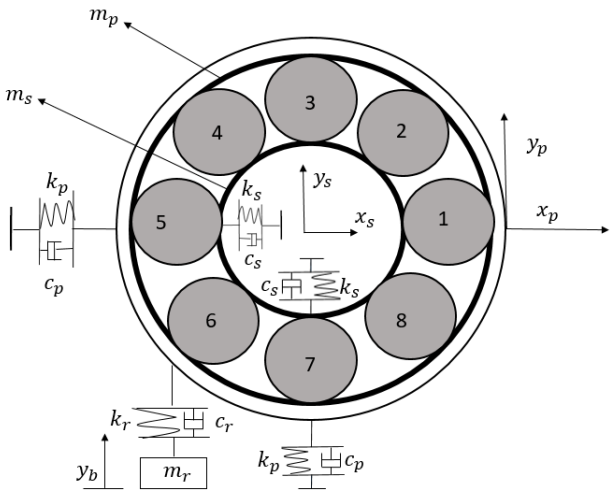

Figure 3.2: Five-DOF Bearing Model (Sawalhi & Randall, 2008)

The following assumptions were made in the development of the model:

- The outer race is stationary while the inner race rotates at constant speed
- All translational motions are in $x - y$ plane and rotations are about z-axis.
- There is no slippage between races and balls, and the balls always remain in contact with the races
- The contact between the ball and inner race, and ball and outer race is considered as surface contact which follows Hertzian contact model

- There is constant angular separation between balls due to an ideal massless cage, and the balls are massless (Sawalhi, 2007)

The general equations of motion for this rotor-bearing system needed for modelling can be expressed by

$$m_s\ddot{x_s} + c_s\dot{x_s} + k_s(x_s) + (f_x((x_s - x_p), \omega_s, dt)) = 0, \tag{3.1}$$

$$m_s\ddot{y_s} + c_s\dot{y_s} + k_s(y_s) + (f_x((y_s - y_p), \omega_s, dt)) = 0, \tag{3.2}$$

$$m_p\ddot{x_p} + c_p\dot{x_p} + k_p(x_p) + (f_x((x_s - x_p), \omega_s, dt)) = 0, \tag{3.3}$$

$$\begin{aligned} &m_p\ddot{y_p} + (c_p + c_r)\dot{y_p} + (k_p + k_r)y_p - k_r y_b - c_r\dot{y_b} \\ &+ (f_y((y_s - y_p), \omega_s, dt)) = 0 \end{aligned} \tag{3.4}$$

$$m_r\ddot{y_b} + c_r(\dot{y_b} - \dot{y_p}) + k_r(y_b - y_p) = 0, \tag{3.5}$$

where m_s denotes the mass of shaft, c_s denotes damping of shaft, k_s is stiffness of shaft, m_p is mass of pedestal, c_p is damping of pedestal, k_p is stiffness of pedestal, m_r is mass of resonance changer, c_r is its damping and k_r is its stiffness, ω_s is shaft rotational speed, y_b is measured vibration response, x_s and y_s denote the shaft's degree of freedom, x_p and y_p are the outer race degree of freedom.

The overall contact deformation (compression) δ_j for the j^{th} rolling element can be expressed as

$$\delta_j = (x_s - x_p)\cos\theta_j + (y_s - y_p)\sin\theta_j - c - \beta_j C_d, \tag{3.6}$$

where, β_j is the fault switch, c is the clearance, and C_d is the depth of spall. Since the compression occurs only when δ_j is positive, a contact state γ_j is introduced as

$$\gamma_j = \begin{cases} 1, & \text{if } \delta_j > 0. \\ 0, & \text{otherwise.} \end{cases} \tag{3.7}$$

The angular positions of the rolling elements ϕ_j, are functions of previous cage position ϕ_o, cage speed ω_c (calculated from geometry and shaft speed ω_s assuming no slippage) and time increment dt and is expressed as (Deshpande, 2014)

$$\phi_j = \frac{2\pi(j-1)}{nb} + \omega_c dt + \phi_o, \tag{3.8}$$

where j is the rolling element and n_b is number of balls. The cage speed ω_c is given by

$$\omega_c = \left(1 - \frac{D_p}{D_b}\right) \frac{\omega_s}{2}, \tag{3.9}$$

where D_p is pitch diameter and D_b is ball diameter.

Using Hertzian theory for non-linear stiffness, the ball raceway contact force is given by

$$f = k_b \delta^n, \tag{3.10}$$

where, k_b is load deflection factor, depends on the contact geometry and the elastic contacts of the material, and exponent n= 1.5 for ball bearings and n= 1.1 for roller bearings.

The load deflection factor is given by

$$k_b = \frac{48EI}{L^3}, \tag{3.11}$$

where, L is the length of the beam E is Young's Modulus and I is the moment of inertia. The total force for a ball bearing with n_b balls is calculated by summing the contact forces in the x and y directions and is given by

$$f_x = k_b \sum_{j=1}^{n_b} \gamma_j \delta_j^{1.5} \cos\phi_j, \tag{3.12}$$

$$f_y = k_b \sum_{j=1}^{n_b} \gamma_j \delta_j^{1.5} \sin\phi_j, \tag{3.13}$$

where, n_b is number of balls of the bearing, γ_j is the contact state of the overall contact deformation δ_j of the jth rolling element, while ϕ_j is the angular position of the rolling elements.

3.2.2 Modelling of Outer Race Fault

A spall of a depth (C_d) over an angular distance of ($\triangle\phi_d$) is modelled using the fault switch β_j to simulate the contact loss at a defined angular position (ϕ_d). This in turn defines the spall region as a step function (Sawalhi, 2007). The outer race spall normally occurs in the load zone and is fixed in location between ϕ_d and $\phi_d + \triangle\phi_d$ as shown in Figure 3.3.

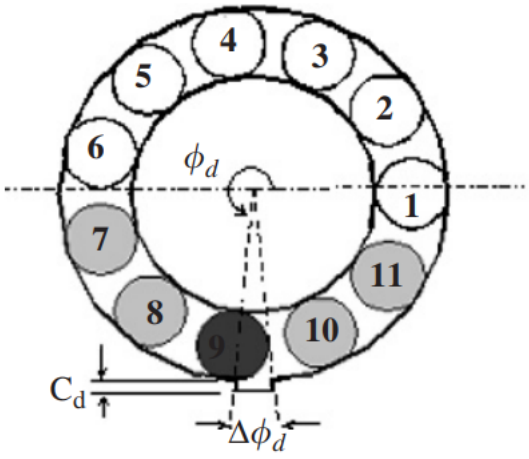

Figure 3.3: Spall definition on outer race (Sawalhi & Randall, 2008)

3.2.3 Modelling of Inner Race Fault

A spall on the inner race rotates at the same speed as the rotor and therefore in this case, $\phi_d = \omega_s t + \phi_{do}$. For both the outer and inner race fault, the fault switch β_j is

defined as

$$\beta_j = \begin{cases} 1, & \text{if } \phi_d < \phi_j < \phi_d + \triangle\phi_d. \\ 0, & \text{otherwise.} \end{cases} \tag{3.14}$$

3.2.4 Development of Particle Swarm Optimisation Algorithm in Parameter Identification

Particle Swarm Optimisation is a swarm intelligence optimisation algorithm that simulates social behaviour such as birds flocking or fish schooling in order to achieve precise objectives in a multi-dimensional space. This method was first introduced by Eberhart and Kennedy (1995).

In PSO, the population is referred to as a swarm and an individual is called particle. Similar to evolutionary algorithms, PSO performs searches using a swarm of particles that are updated from one iteration to another as they travel through a search space. Each swarm of particles has a position vector and a velocity vector, which represent respectively the potential solution of the problem and the direction in the search space (Singh & Tiwari, 2018). Particle Swarm Optimisation remembers both the best position found by all particles and that by each particle in the search process. In order to determine the optimal solution, the particle's velocity is updated by the following equation

$$v_{k+1} = \omega v_k + c_1 r_1 (p_{best} - x_k) + c_2 r_2 (g_{best} - x_k), \tag{3.15}$$

where, ω is the inertia, k is the iteration number, x_k is the current particle position, v_k is current velocity of the particle, p_{best} is the optimal particle position, g_{best} is optimal swarm position, c_1 and c_2 are the learning factors describing the cognitive and social behaviour of the system, and r_1 and r_2 are random numbers between 0 and 1 (Ge et al., 2019).

The particle's position is updated by

$$x_{k+1} = x_k + v_{k+1}. \tag{3.16}$$

The velocity of the particle was adjusted based on its best performance and the best performance of the best particle and this is bound to a maximum and minimum value beyond which the particle should not exceed. The algorithm continues to perform repeated applications of updating equation until a stopping criterion is reached.

To solve the problem of parameter estimation, the bearing parameters to be estimated were listed in a state vector called $parName$ given by

$$parName = 'ms';' mp';' mr';' ks';' kp';' kr';' kb';' cs';' cp';' cr';' c';' slip' \tag{3.17}$$

where the ms, mp and mr are mass of shaft, pedestal and resonance changer respectively, ks, kp and kr are stiffness of shaft, pedestal and resonance changer respectively, kb is load deflection factor, cs, cp and cr are damping of shaft, pedestal and resonance respectively, c is clearance and $slip$ is slippage.

Figure 3.4 shows the steps that were carried out in development of the PSO algorithm and were also listed in Lei et al. (2018). The steps in the flow chart are explained in details in the sections below.

1. Set PSO parameters. The parameters such as population size, initial inertia etc and their corresponding values were initialised as listed in Table 3.1. These parameters have been referenced in several researches (Alam et al., 2015) as the ones that give optimal results

2. Initialize a population of particles with random position and velocities. A

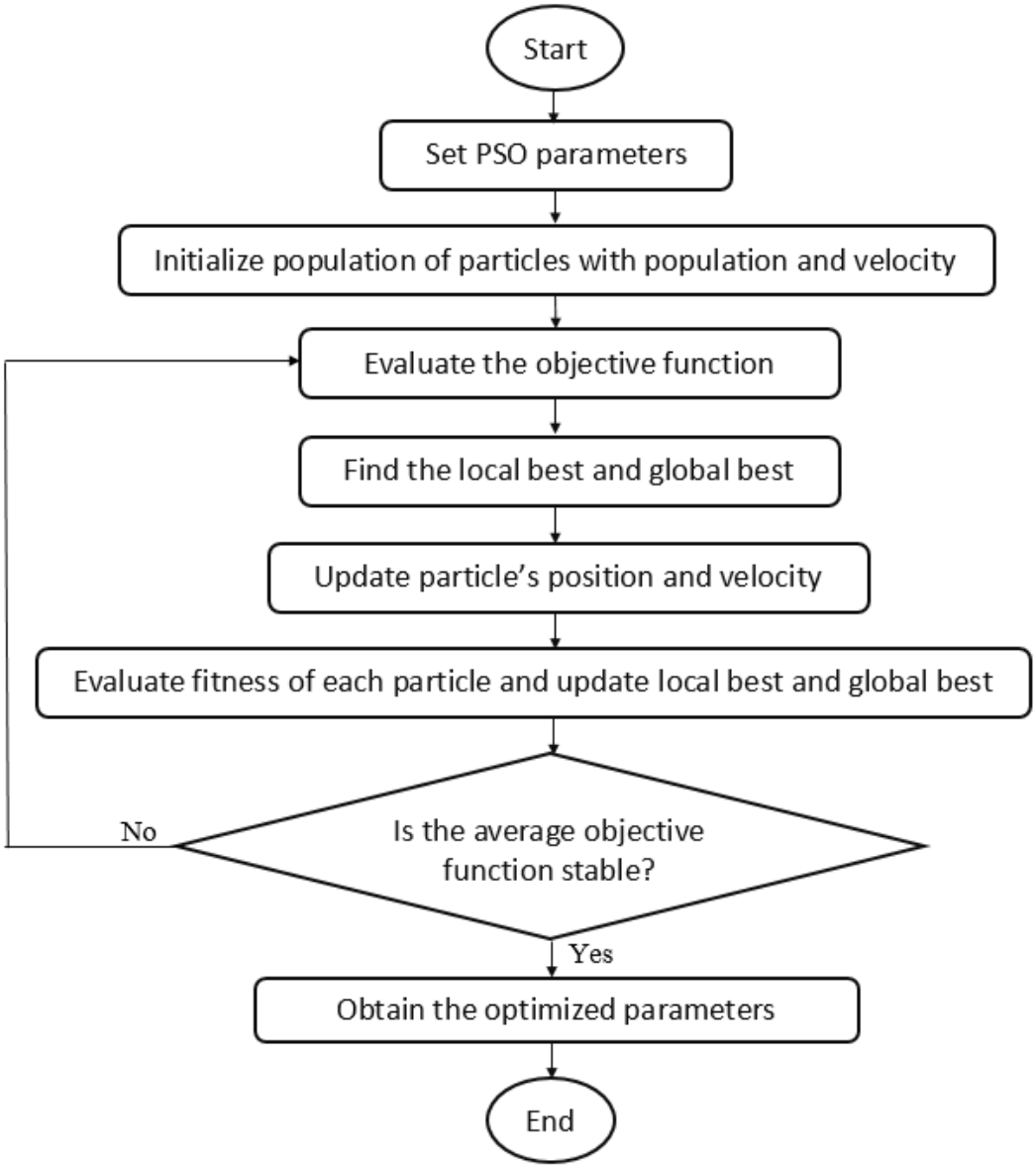

Figure 3.4: Flowchart of PSO algorithm (Jin et al., 2014)

population of particles was initialized using the following equation

$$p = rand(pSize, Dim) \tag{3.18}$$

where p are uniformly distributed values from 0 to 1, $pSize$ and Dim are the population size and dimension respectively. The random values were then

converted to the relevant range between $xmin$ and $xmax$ in every dimension. This was done in a 2-dimensional problem space. The particle's velocity was bound to a maximum and minimum value beyond which the particle should not exceed. Limit on the search space was applied using a limiting maximum velocity $vmax$ which is given by

$$vmax = .06 * (xmax - xmin) \tag{3.19}$$

where $xmax$ and $xmin$ are the maximum and minimum values of the parameters to be estimated respectively.

3. Evaluate the objective function. The objective function was set to be the mean squared error (MSE) between the desired and measured vibration response. The objective function is given as

$$MSE = \frac{1}{N} \sum_{k=1}^{N} \left[X(k) - \hat{X}(k) \right]^2 \tag{3.20}$$

where N is the sampling number, $X(k)$ and $\hat{X}(k)$ are real and estimated values of state vector representing RMS, kurtosis and peak amplitude and peak frequency at time k, respectively. The goal is to reduce the MSE between the desired and measured vibration response in order to obtain optimal bearing parameters.

4. Find the local best and global best. These represent the optimal values of particle and swarm position and were compared with those of the current population and those results which are better than the rest were retained.

5. For each particle, the particle position and velocity were updated using the Eqs 3.16 and 3.15 respectively to generate a new swarm

6. Memory updating- The fitness value of the newly updated particles was

evaluated and then the local best and global best were updated

7. Termination criteria examination. If the objective function was not met, the algorithm returns to step 3, else it proceeds to step 7

8. Obtain optimized parameters. The global best position in the swarm was selected as the ultimate solution and this revealed the optimized bearing parameters.

The main goal of the PSO algorithm is to find the optimal bearing parameters that minimize the objective function (Lin et al., 2016). Therefore, the convergence of the algorithm is dependent on the selection of the parameters such as inertia factor of the particle, population size, maximum velocity and so on.

Table 3.1: PSO Parameters

Parameters	**Symbol**	**Value**
Population size	p	25
Initial inertia	w_{in}	0.8
Final inertia	w_f	0.3
Self-confidence factor	c_1	3
Swarm confidence factor	c_2	2

3.2.5 Simulation Setup

MATLAB/Simulink environment was used to come up with the bearing model where the equations of motion are solved. This model was created using parameters from Sawalhi and Randall (2008) and was used to diagnose bearing faults of outer race and inner race. The contact force was implemented as a Matlab function block in SIMULINK environment. The function block had various inputs and outputs which correspond to the equations previously listed above. The Function block is seen in Figure 3.5. The inputs to the function block include contact angle (phi0), time

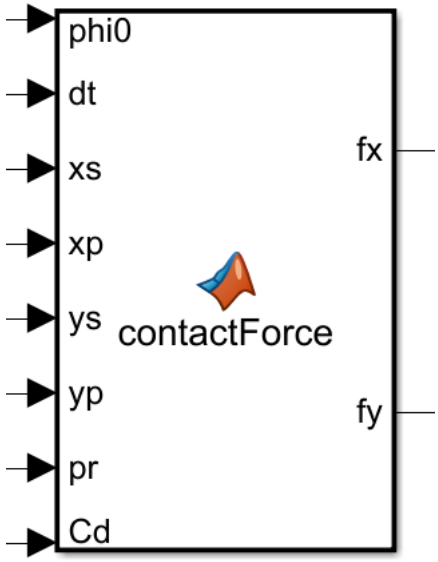

Figure 3.5: Matlab Function Block

increment (dt), xs, xp, ys and yp, which are the shaft and outer race's degrees of freedom , pr which includes several variables such as number of balls (nb), cage speed (wc), slippage (slip), clearance (c), location of outer race fault (phid), width of outer race fault (dph), load deflection factor (kb) and finally the fault depth denoted as Cd in the function block. The outputs of the function block are fx and fy which denote contact force in the x and y direction respectively. The outputs are fed to block parameters of addition or subtraction depending on the equations. Moreover, mass, spring and damping are modeled using gains and integrals accordingly. The bearing model was dynamically updated as the simulation proceeded. The complete simulink model is shown as a figure in Appendix B.

The physical specifications of the bearing-pedestal system that were used to come up with the inital bearing model are listed in Table 3.2. The pedestal stiffness was chosen to correspond to the 174-Hz frequency (the casing's lowest natural frequency in the vertical direction (Sawalhi & Randall, 2008)). The sprung mass stiffness is chosen to provide a typical high frequency resonance of 15 kHz. The rolling elements'

damping was set to 5%, while the rolling elements' friction was set to 5%. The pedestal's damping was set at 8%, while the sprung mass system's damping was set to 5%.

Table 3.2: Search Range of Bearing Parameters and their Initial Values (Sawalhi & Randall, 2008)

Parameters	**Specified Search Range**	**Initial Values**
Mass of shaft	$0.01 \leq m_s \leq 2$	0.5134
Mass of pedestal	$0.01 \leq m_p \leq 2$	1.752
Mass of resonator	$0.01 \leq m_r \leq 2$	0.8392
Stiffness of shaft	$1 \times 10^6 \leq k_s \leq 1 \times 10^8$	9.2325×10^7
Stiffness of pedestal	$1 \times 10^6 \leq k_p \leq 1 \times 10^8$	1.987×10^7
Stiffness of resonator	$1 \times 10^8 \leq k_r \leq 1 \times 10^{10}$	4.291×10^9
Load distribution factor	$1 \times 10^{11} \leq k_b \leq 1 \times 10^{12}$	6.918×10^{11}
Damping of shaft	$2 \times 10^3 \leq c_s \leq 1 \times 10^4$	4.917×10^3
Damping of pedestal	$2 \times 10^3 \leq c_p \leq 1 \times 10^4$	6.3123×10^3
Damping of resonator	$2 \times 10^3 \leq c_r \leq 1 \times 10^4$	5.4230×10^7
Clearance	$1 \times 10^{-7} \leq c \leq 1 \times 10^{-5}$	8.1927×10^{-7}
Slippage	$0.008 \leq slip \leq 0.02$	0.0198

The model was also used in the PSO algorithm to set up the objective function and identify parameters of the bearing baseline conditions. Once the optimal parameters were obtained, the model was then simulated with these parameters to obtain the bearing response with different fault conditions.

The estimated parameters were used to simulate outer race fault and inner race fault and the accuracy of the model with parameters estimated by PSO was determined by comparing the characteristic defect frequencies (Cd) of simulation to the corresponding theoretical defect frequencies (Td) as shown in Equation 3.21

$$\text{Accuracy}(\%) = 100 - \left(\frac{Cd - Td}{Cd} \times 100 \right) \tag{3.21}$$

Frequency was used as opposed to amplitude because amplitudes vary greatly due to presence of noise in the system. The model was then validated by experimental

data from two publicly available datasets.

3.3 Prognostics

Figure 3.6 is a block diagram summarizing the workflow of the prognostics section.

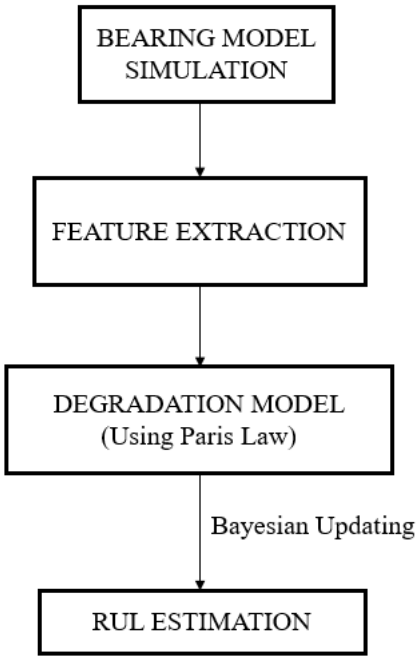

Figure 3.6: Block diagram representation of RUL Framework

First of all, a simulation of the bearing degradation process was done in Matlab using the developed bearing model employing the estimated model parameters to generate vibration data. Statistical features such as RMS and Kurtosis were then extracted from the simulation data. A quantitative assessment of the statistical features was done. Root Mean Square (RMS) was selected as the most suitable health indicator and used in the bearing degradation model to estimate the remaining useful life of the bearing.

3.3.1 Simulation of the Bearing Degradation Process

Simulation of the vibration signals that represent the degradation process of rolling element bearings was carried out. The estimated parameters that yielded a higher accuracy acted as inputs to the SIMULINK model , together with the geometric data from CWRU Dataset ,to generate vibration degradation data The defect width was varied from 0 to 3 mm with 50 simulations carried out to obtain their vibration signals. The parameters of the bearing used in the simulation are as shown in Table 3.3.

Table 3.3: Bearing Geometric Data

Bearing Specification	Value
Outer diameter (mm)	25
Inner diameter(mm)	0.8
Pitch diameter(mm)	29.05
Ball diameter (mm)	6.75
Number of balls	8
Contact angle (degree)	0
Sampling frequency(kHz)	25.6

‘

3.3.2 Statistical Feature Extraction

Feature extraction of the simulated vibration signals was carried out in time domain. Time domain methods usually involve statistical features that are sensitive to impulsive oscillation, such as kurtosis, skewness, peak-peak (P-P), RMS, and sample variance. The 4 domain statistical features that were used as potential health indicators of the bearing are RMS, kurtosis, skewness and crest factor.

3.3.2.1 Root Mean Square (RMS)

The RMS of a signal (x) is given by

$$RMS(x) = \sqrt{\frac{1}{N}\sum_{k=1}^{N} x_k^2}, \tag{3.22}$$

where N is the number of samples in the signal and x_k is the discrete value at time index k. RMS values of vibration signals describe the energy content of a signal and can be used to monitor the overall vibration level of bearings due to the fact that the overall vibration level typically increases as the bearing deteriorates Sawalhi, 2007. Root Mean Square (RMS) is one of the commonly used statistical parameters (Ahmad et al., 2018; Li et al., 2015) to indicate the health of a bearing and was used as a prediction indicator in this thesis.

3.3.2.2 Kurtosis

The kurtosis of a random signal (x) is given by

$$KU(x) = \sqrt{\frac{\frac{1}{N}\sum_{k=1}^{N}(x_k - \mu)^4}{\sigma^4}}, \tag{3.23}$$

where N is the number of samples in the signal, x_k is the discrete value at time index k, μ is the mean and σ is the standard deviation. Kurtosis is a measure of impulsiveness in a signal and hence a good indicator of a fault. A healthy bearing has a kurtosis value of 3 but the value increases as the bearing fault increases.

3.3.2.3 Crest Factor

The crest factor of a signal (x) is given by the peak value divided by RMS as expressed in the following equation

$$CF = \frac{\max(x_k)}{RMS}, \tag{3.24}$$

where x_k is the discrete value at time index k and RMS is the root mean square value of the signal. The crest factor can provide an early warning for faults when they develop.

3.3.2.4 Skewness

The skewness of a signal measures the asymmetry of a signal distribution. It is given by

$$(SK) = \sqrt{\frac{\frac{1}{N}\sum_{k=1}^{N}(x_k - \mu)^3}{\sigma^3}}, \tag{3.25}$$

where N is the number of samples in the signal, x_k is the discrete value at time index k, μ is the mean, and σ is the standard deviation. The level of skewness can be impacted by faults in a bearing.

3.3.3 Metrics for Health Indicators

A quantitative assesment of the above mentioned health indicators was done using three metrics; monotonicity (Javed et al., 2015; Lei et al., 2018), robustness (Zhang et al., 2016), and trendability (Lei et al., 2018; Zhang et al., 2016).

3.3.3.1 Monotonicity

Monotonicity measures whether the Health Indicator (HI) is trending upwards or downwards (Javed et al., 2015; Lei et al., 2018). It is given by

$$\text{Mon(X)} = \frac{1}{K-1}\left|\text{No. of}\left(\frac{d}{dx}\right) > 0 - \text{ No. of}\left(\frac{d}{dx}\right) < 0\right|, \tag{3.26}$$

where $X = x_{kk=1:K}$ is the HI sequence with x_k representing the HI value at time t_k, K is the total number of the HI values included in the sequence, $d/dx = x_{k+1} - x_k$ denotes the difference of the HI sequence, No. of $\left(\frac{d}{dx} > 0\right)$ and No. of $\left(\frac{d}{dx} < 0\right)$ represent the number of the positive differences and the negative differences, respectively. The value of Mon (X) changes from 0 to 1 due to the absolute difference

in positive and negative derivatives of X and a higher value of Mon(X) means that the HI has better performance monotonically.

3.3.3.2 Robustness

This metric measures the ability of the HI to withstand random fluctuations caused by measurement noise, stochasticity of the degradation processes and the alteration of operating conditions (Zhang et al., 2016). The equation is given by

$$\text{Rob}(X) = \frac{1}{K}\sum_{k=1}^{K} \exp\left(-\left|\frac{x_k - x_k^T}{x_k}\right|\right), \tag{3.27}$$

where x_k is the indicator value of X at t_k, and x_k^T is the mean trend value of the HI at t_k which is acquired through smoothing methods.

3.3.3.3 Trendability

A bearing is likely to degrade more with use as time passes. Due to this, the trendability is a metric used to measure the correlation between degradation trend of a HI with the operating time (Lei et al., 2018; Zhang et al., 2016). Trendability is given by

$$\text{Tre(X,T)} = \frac{K(sum_{k=1}^{K} x_k t_k) - (\sum_{k=1}^{K} x_k)(sum_{k=1}^{K} t_k)}{\sqrt{\left[\sum_{k=1}^{K} x_k^2 - (sum_{k=1}^{K} x_k)^2\right]\left[\sum_{k=1}^{K} t_k^2 - (sum_{k=1}^{K} t_k)^2\right]}}, \tag{3.28}$$

where, t_k is the k^{th} value of time and x_k is the value of the HI at time t_k. The values range from -1 to +1 where -1 indicates a strong negative correlation and +1 indicates a strong positive correlation.

3.3.4 Paris Law Degradation Model

Once an assessment of the health indicators was conducted, the extracted features of best performing health indicator were used as input of the Paris model for bearing

degradation process prediction.

Paris Law describes the rate of bearing crack growth with the following equation

$$\frac{da}{dN} = C(\Delta k^m), \tag{3.29}$$

where, a is the crack size at the number of cycles N,$\Delta k = \gamma\sigma\sqrt{\pi a}$,$\sigma$ is the cyclic load amplitude and m, c and γ are material constants. Henceforth, a will be referred to as the health state of the bearing. The growth of the crack is governed by the model parameters. The size of the crack at future cycles can be predicted by substituting the identified parameters with future loading conditions. In order to integrate Eq.3.29, the initial condition (initial health state, $a0$) is required. When the initial health state is also unknown, it has to be included as unknown parameters. Therefore, the Paris model has three unknown parameters $m; C; a0$ The three parameters were identified by minimizing an objective function using non-linear least squares (NLS). The objective function is the mean square error between measurements and model simulation. To obtain the objective function, the ordinary differential equation in Eq. 3.29 is first solved for a as

$$a = \left[N.C(1 - \frac{m}{2})(\Delta\sigma\sqrt{\pi})^m + a0^{\left(1-\frac{m}{2}\right)}\right]^{\frac{2}{2-m}} \tag{3.30}$$

, $a0$ is the initial half crack size, a is the half crack size at the number of cycles C is based on the initial conditions, being determined by solving Eq. 3.30 with initial values $a = a1$ and $N = 0$. The goal was to minimize the error between the measurements and the model. The unknown parameters were identified using the Non Least Squares (NLS) minimization routine. The simulated data was used to identify (or calibrate) model parameters. Once the model parameters were identified, they were then used to predict the future behavior of the damage (Lee et al., 2014).

3.3.5 Implementation with Bayesian Method

Bayesian inference was used to estimate and update unknown parameters based on measured degradation data using health monitoring systems. The unknown model parameters were represented as a probability density function (PDF), which was updated with more data and prior knowledge or information. The more data was available, the more accurate estimation of model parameter was possible. Once the PDF of model parameters was obtained, it could be used to predict the remaining useful life before the system fails. Since the model parameters are given in the form of PDF, the remaining useful life will also be in the form of PDF

In this thesis, the Bayes method is used in the context of Bayesian inference. To estimate the probability of A given B, the Bayes' theorem is given by

$$P(A/B) = \frac{P(B/A)P(A)}{P(B)} \tag{3.31}$$

where $P(B/A)$ is the probability of B given A, Event A is the hypothesis, event B is called evidence,$P(A)$ is the prior and $P(A/B)$ is called the posterior.

3.3.6 Likelihood and Prior Distribution

According to the Bayesian method explained above, the likelihood and prior distribution should be defined in order to obtain the posterior distribution. In this section, normal and uniform distributions are employed for the likelihood and prior distribution, respectively. The likelihood function can be expressed in the following form

$$f(y_k|m_k^i, C_k^i) = \frac{1}{y_k\sqrt{2\pi}\zeta_k^i} exp\left[-\frac{1}{2}\left(\frac{\ln y_k - \eta_k^i}{\zeta_k^i}\right)^2\right], i = 1....n_s \tag{3.32}$$

where, $\zeta_k^i = \sqrt{\ln\left[1 + \left(\frac{(\sigma}{a_k^i(m_k^i C_k^i)}\right)^2\right]}$, is standard deviation and $\eta_k^i = \ln\left[a_k^i(m_k^i C_k^i)\right] - \frac{1}{2}(\zeta_k^i)^2$ denotes mean of lognormal distribution respectively. In the above equations, $a_k^i(m_k^i C_k^i)$ is the model prediction from the bearing crack growth equation at time t_k with given model parameters m_k^i and C_k^i

Also, the prior/initial distributions of the parameters are assumed as normal distributions as

$$f(m) = N(4, 0.2^2), f(\log \mathrm{C}) = N(-23, 1.1^2) \tag{3.33}$$

,

3.3.7 RUL Prediction

In order to calculate the RUL, it was necessary to find the time cycle when the level of degradation reaches the threshold. The degradation model was given in such a way that the degradation can explicitly be calculated for a given cycle. However, calculating the time cycle when the degradation reaches a certain level is not straightforward as the relation is nonlinear and implicit. Therefore, in order to find the end-of-life, the following nonlinear equation had to be solved to find time cycle t_{EOL}

$$y_{threshold} - z(t_{EOL}; \hat{\theta}) = 0 \tag{3.34}$$

In general, the above nonlinear equation was solved numerically using Newton-Raphson iterative method. In MATLAB code, the function solve was used to find the time cycle t_{EOL} that satisfies the above relation, where the solution t_{EOL} is called the end-of-life (EOL). The remaining useful life (RUL) can be determined from $t_{RUL} = t_{EOL} - t_{current}$. Since $z(t_{EOL}; \hat{\theta})$ is a monotonic function, the above equation will have a unique solution.

CHAPTER FOUR

RESULTS AND DISCUSSION

4.1 Overview

This aim of this section is to highlight the results from the proposed model in bearing diagnostics and prognostics. Validity of the approach that was employed was investigated using two publicly available datasets and the results from estimation of Remaining Useful Life were stated.

4.2 Case Study 1: Case Western Reserve University (CWRU) Dataset

4.2.1 Experimental Setup and Dataset

This case study feature bearing dataset provided by "Case Western Reserve University Bearing Data Center" (n.d.). The deep groove balling bearing 6205-2RS JEM SKF was used in the experiment. The whole experimental rig shown in Figure 4.1 consists of a two horsepower three-phase induction motor, a torque transducer, and a dynamometer. This ball-bearing vibration dataset is collected from a 2-hp reliance electric motor and the accelerators are installed at the drive end, the fan end, and the base, respectively. The sampling frequency used is 12 kHz under different loads, ranging from 0 to 3 hp. There are three fault types of drive end bearing, which are: inner race fault (IF), ball fault (BF), and outer race fault (OF). Moreover, single point faults of three different sizes (0.18mm, 0.36mm and 0.54 mm) for each fault type are introduced using elecro-discharge machining. The motor speed is 1797 rpm.

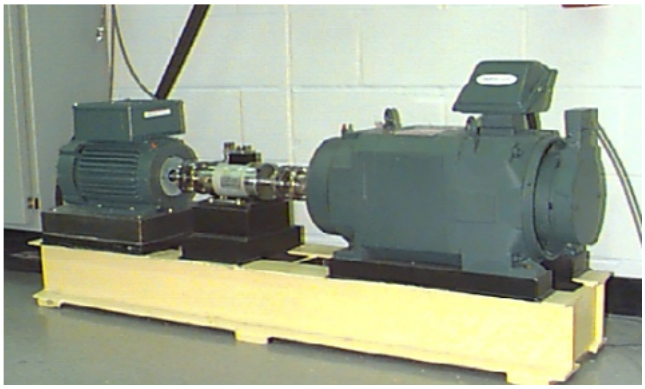

Figure 4.1: Apparatus for the bearing vibration signal collection of the CWRU bearing dataset ("Case Western Reserve University Bearing Data Center", n.d.)

4.2.2 Bearing Modelling and Simulation

The bearing geometric data shown in Table 4.1 was obtained from the CWRU Bearing Data Center and it represents the dimensions of the bearings used in the experimental data. This data was also used to calculate theoretical characteristic frequencies using Equations 2.1-2.3. The theoretical characteristic defect frequencies for this set of data are listed in Table 4.2. The bearing model was developed in SIMULINK used parameters obtained from Sawalhi and Randall (2008) and this geometric data.

This model was used to simulate faults in the inner and outer races and the accuracy of the model was determined by the comparing the characteristic defect frequencies in the simulated signal with the corresponding theoretical frequencies.

Table 4.1: Bearing Geometric Data for CWRU Dataset

Bearing Specification	Value
Outer diameter (mm)	52
Inner diameter(mm)	25
Pitch diameter(mm)	39.04
Ball diameter (mm)	7.04
Number of balls	9
Contact angle (degree)	0

Table 4.2: Bearing Characteristic Frequencies of CWRU Dataset

Parameters	Value
Ball Pass Frequency of Inner Race (BPFI)	162.19
Ball Pass Frequency of Outer Race (BPFO)	107.34
Ball Spin Frequency (BSF)	70.59
Fundamental Train Frequency (FTF)	11.93
Number of balls	8
Contact angle (degree)	0

Figure 4.2 shows the simulated vibration response of bearing with outer race defect with the time-domain waveform and envelope spectrum. It can be observed that the vibration signal has periodic characteristic. This is due to impact vibration produced by the ball as it moves over the defect. Thus the time-domain signal (a) depicts a series of attenuation vibrations. It can also be observed that the envelope spectrum of a single outer race fault signal contains the fault characteristic frequency of the bearing outer race (105.7 Hz, very close to the theoretical value of 107.34 Hz) and its second and third harmonic frequencies (216.5 Hz and 322.2 Hz, respectively). This shows that the model is fairly accurate by 98.5% .

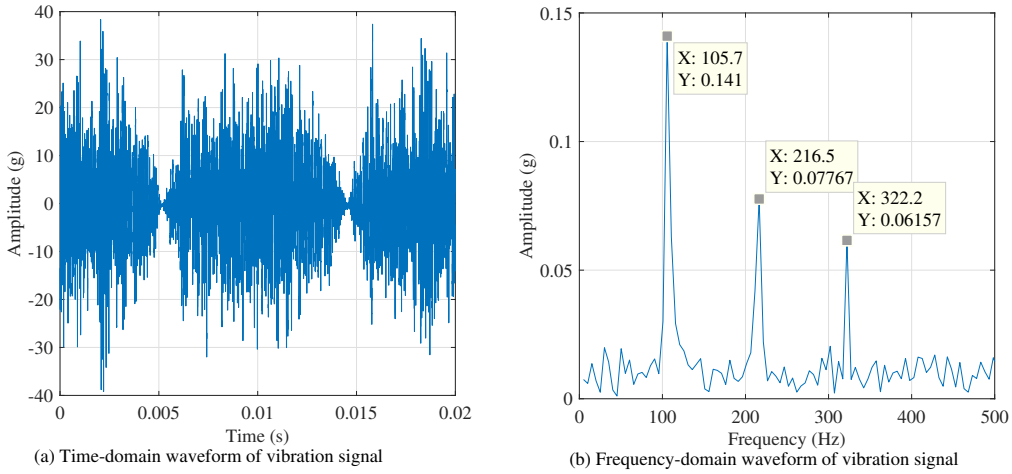

Figure 4.2: Simulated vibration response of bearing with outer race defect

Figure 4.3 shows the simulated vibration response of bearing with inner race defect with the time-domain waveform and envelope spectrum. Several spectral lines of varying amplitudes can be observed. The envelope spectrum of a single inner ring fault signal features several spectral lines of gradually decreasing amplitudes appearing as sinusoidal modulation. These amplitudes occur at multiple frequencies of each order. According to the spectrum, the characteristic frequency of defect is 163.9 Hz while the first and second order harmonics appear at 324.4 Hz and 484.9 Hz, respectively. According to Table 4.2, the theoretical fault characteristic frequency of the inner ring was 162.19 Hz and when compared to the simulated signal, it gives an accuracy of 98.32%. These results obtained from the simulated vibration responses show that the bearing model created is able to accurately diagnose bearing faults.

The simulink model was called within the PSO algorithm to set up the objective function. Once these optimal parameters were obtained, the model was simulated once again, using the estimated parameters to obtain the bearing response of different fault conditions. Table 4.3 shows the results obtained from optimization of the bearing parameters. The results obtained show that the bearing parameters values

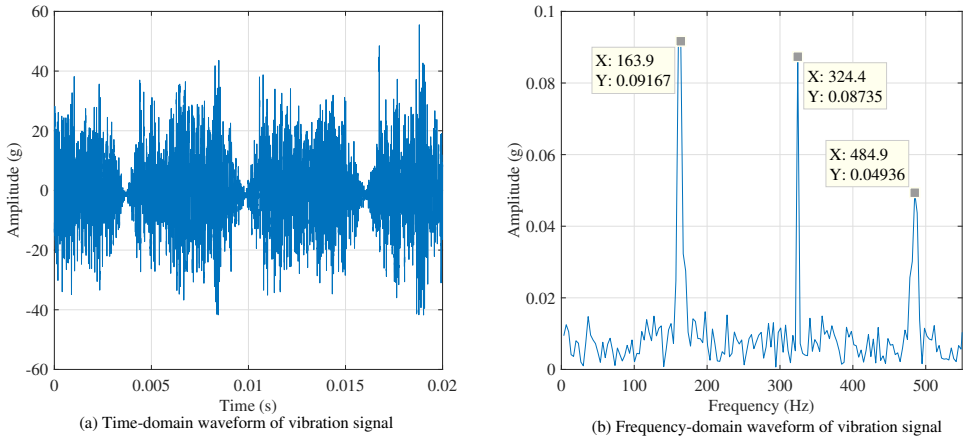

(a) Time-domain waveform of vibration signal

(b) Frequency-domain waveform of vibration signal

Figure 4.3: Simulated vibration response of bearing with inner race defect

are within the specified search range.

Table 4.3: Search Range of Bearing Parameters and their Estimated Values

Parameters	**Specified Search Range**	**Estimated Values**
Mass of shaft	$0.01 \leq m_s \leq 2$	0.1542
Mass of pedestal	$0.01 \leq m_p \leq 2$	1.6198
Mass of resonator	$0.01 \leq m_r \leq 2$	0.8461
Stiffness of shaft	$1 \times 10^6 \leq k_s \leq 1 \times 10^8$	8.624×10^7
Stiffness of pedestal	$1 \times 10^6 \leq k_p \leq 1 \times 10^8$	1.125×10^7
Stiffness of resonator	$1 \times 10^8 \leq k_r \leq 1 \times 10^{10}$	2.974×10^9
Load distribution factor	$1 \times 10^{11} \leq k_b \leq 1 \times 10^{12}$	8.146×10^{11}
Damping of shaft	$2 \times 10^3 \leq c_s \leq 1 \times 10^4$	5.9631×10^3
Damping of pedestal	$2 \times 10^3 \leq c_p \leq 1 \times 10^4$	7.3502×10^3
Damping of resonator	$2 \times 10^3 \leq c_r \leq 1 \times 10^4$	5.2647×10^7
Clearance	$1 \times 10^{-7} \leq c \leq 1 \times 10^{-5}$	8.4096×10^{-7}
Slippage	$0.008 \leq slip \leq 0.02$	0.0159

The bearing model with estimated bearing parameters was validated in Fig. 4.4 by comparing the vibration response of the model with estimated parameters to vibration response of experimental data obtained from CWRU bearing dataset. There was some similarity in the periodic characteristic in both the time-domain

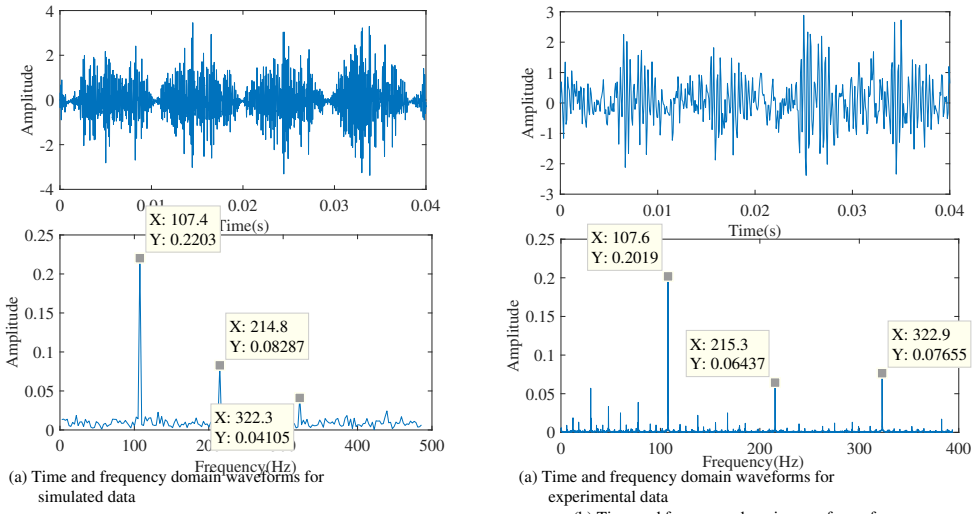

Figure 4.4: Vibration response of outer race fault of simulated signal (a) vs experimental data (b)

and envelope spectrum waveforms of simulated and experimental signals. The experimental data reveals more background noise compared to the simulated one. The characteristic frequency spectra of the simulated signal is 107.4 Hz while that of the experimental data is 107.6 Hz. This shows that the vibration response bearing model that has parameters estimated through PSO because compares closely to the experimental data characteristic frequency and the theoretical ball pass frequency of inner race which is 107.34 Hz. The accuracy of the model with estimated parameters is 99.96%. The results show an improvement in the accuracy when the bearing parameters are estimated using particle swarm optimisation.

Figure 4.5 also shows validation of vibration response of the model with estimated parameters compared to experimental data obtained from CWRU bearing dataset for a bearing with inner race fault. A peak could be seen at around 20 Hz in the experimental data which can be explained by the shaft rotational frequency. Another peak was present at 161.9 Hz. The characteristic defect frequency of simulated data is 161.1Hz while that of experimental data is 161.9Hz. Moreover, higher order frequencies are present in both the simulated and experimental data. However, the

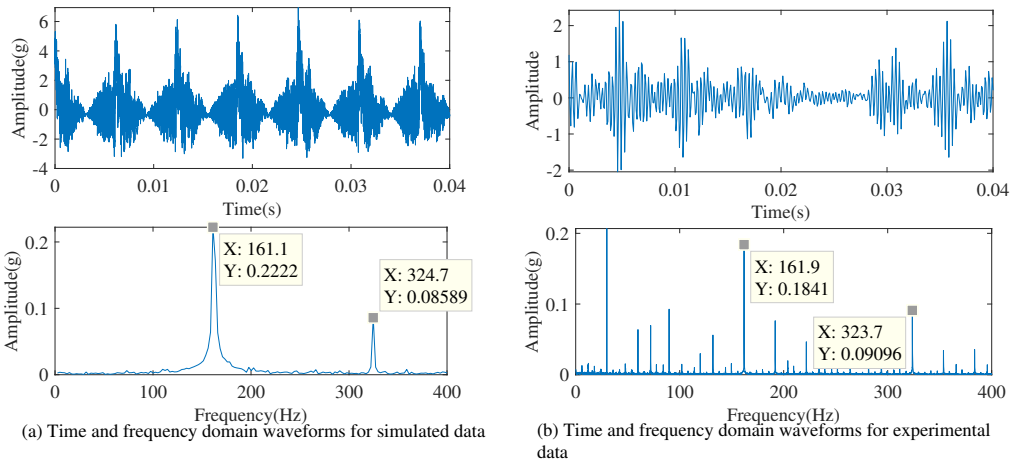

Figure 4.5: Vibration response of inner race fault of simulated signal (a) vs experimental data (b)

experimental data has many intermediate peaks when compared to the simulated data. On calculating the accuracy, it was revealed that the model with bearing parameters estimated via PSO gives an accuracy of 99.38%.

From the above results, it was easily observed from Figure 4.4 and Figure 4.5 that parameter estimation with PSO algorithm has yielded more accurate models as compared to when the bearing parameters are just assumed. The experimental results indicate that parameter estimation with PSO can accurately recreate the underlying nonlinear, rotor-bearing system. Furthermore, the method enriches the nonlinear, rotor-bearing modeling theory and provides a reliable model for dynamic analysis, design, and fault diagnosis of the rotor-bearing system, which is of practical significance.

4.3 Case Study 2: University Of Paderborn Dataset

4.3.1 Experimental Setup and Dataset

The vibration signals used in this section are provided by the Bearing Data Center at the "University of Paderborn Bearing Data Center" (n.d.).

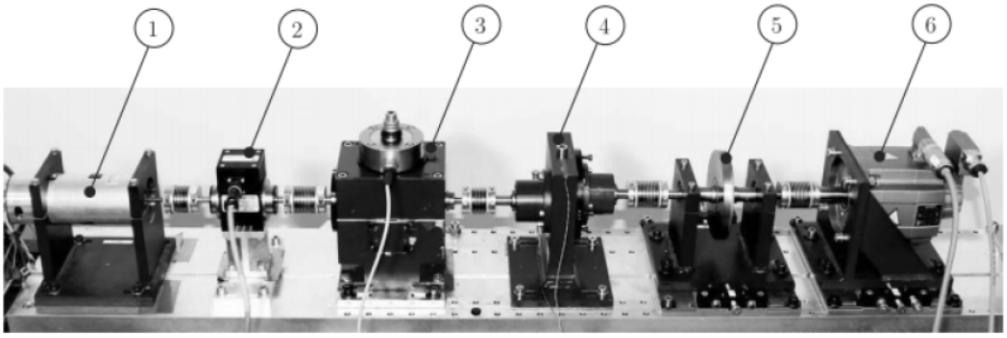

Figure 4.6: Modular test rig for fault diagnosis of rotating machinery("University of Paderborn Bearing Data Center", n.d.)

Figure 4.6 represents the experimental setup of the test rig. The test-rig consists of (1) drive motor (2) torque-measuring shaft, (3) rolling element bearing module, (4) gear module, (5) flywheel and (6) load motor. This bearing dataset consists of the high-resolution vibration data, which are collected from experiments performed on six healthy bearings, and 26 damaged bearing sets. It provides the basis for the development and validation. In this research, two vibration datasets are applied for the validation of the proposed parameter estimation method. One dataset has an outer race fault while the other has an inner race fault. The speed of the motor is 900 RPM.

4.3.2 Bearing Modelling and Simulation Results

The deep groove ball bearing and the simulations also employ the corresponding bearing geometry data.Table 4.4 shows the theoretical characteristic defect frequencies of the bearings used in this experiment calculated from Equations 2.1-2.3. The bearing characteristic frequencies were calculated using the bearing geometric data provided in Table 4.5. The model developed in SIMULINK was used to obtain the simulated signals of the localised faults in inner and outer race. These characteristic frequencies observed in the signals were then compared to those obtained from theoretical calculations and then validated with experimental signals.

Table 4.4: Bearing theoretical characteristic frequencies of UoP Dataset

Parameters	**Value**
Ball Pass Frequency of Inner Race (BPFI)	73.94
Ball Pass Frequency of Outer Race (BPF0)	46.06
Ball Spin Frequency (BSF)	30.54
Fundamental Train Frequency (FTF)	35.76
Number of balls	8
Contact angle (degree)	0

Table 4.5: Bearing Geometric Data for UoP Dataset

Bearing Specification	**Value**
Outer diameter (mm)	25
Inner diameter(mm)	0.8
Pitch diameter(mm)	29.05
Ball diameter (mm)	6.75
Number of balls	8
Contact angle (degree)	0

The time-domain waveform and envelope spectrum of simulated vibration signal of outer race defect is shown in Figure 4.7. The figure clearly shows that a defect has occurred in the outer race of a bearing due to the series of attenuation vibrations in

the time-domain signal. Moreover, the frequency spectrum reveals the characteristic frequency of defect of the outer race and its multiple frequencies. These multiple frequencies appear as a series of discrete spectral lines that steadily decrease with the increasing frequency (Sawalhi, 2007). The peak amplitude of the characteristic frequency of defect of outer race is given as 46.83Hz. This value compares favourably with the theoretical characteristic frequency for outer race fault which is 46.06Hz depicting an accuracy of 98.35%.

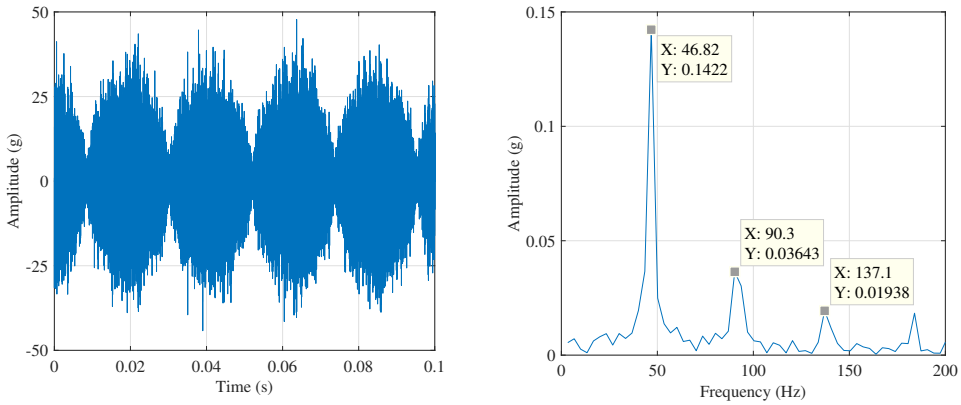

(a) Time-domain waveform of outer race fault

(b) Frequency-domain waveform of outer race fault

Figure 4.7: Simulated signal of rolling element bearing with outer race fault

Figure 4.8 shows the time-domain waveform and envelope spectrum of simulated vibration signal of inner race defect. Similar to the other models, the envelope spectrum features several spectral lines of gradually decreasing amplitudes appearing as sinusoidal modulation. These amplitudes occur at multiple frequencies of each order. According to the spectrum, the characteristic frequency of defect is 75.51 Hz. Compared to the theoretical value of the characteristic defect frequency for inner race which is 73.94 Hz, the model has an accuracy of 97.88%.

These results show that the model that has been created in simulink can be used to accurately simulate bearing faults in the inner and outer races due to the

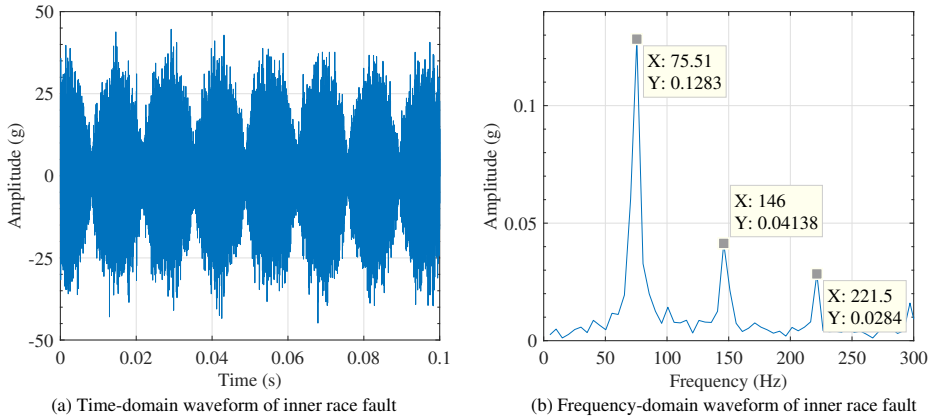

(a) Time-domain waveform of inner race fault

(b) Frequency-domain waveform of inner race fault

Figure 4.8: Simulated signal of rolling element bearing with inner race fault

high accuracy obtained by comparing the characteristic defect frequencies to the theoretical frequencies. Once this model has been created, it was used in the fitness function of the particle swarm optimisation algorithm. Table 4.6 gives the search range and estimated parameters used for University of Paderborn Dataset.

Figure 4.9 shows comparison between simulated signals of the model with estimated parameters and experimental signal of inner race faults depicted, some similarity is visible in the periodic characteristic in both the time-domain and envelope spectrum waveforms of the simulated signal and experimental signal. A peak at a frequency of around 50 Hz can be seen in the experimental data. This is not the peak characteristic defect frequency but it can be explained by the shaft rotational speed of 3000rpm. The experimental data reveals more background noise compared to the simulated one. The other peak frequency of the simulated signal is 73.24 Hz while that of the experimental data is 73.75 Hz. This reveals an improvement in the accuracy of the bearing model whose parameters are estimated through PSO. On calculating the accuracy of the model, it is revealed to be at 99.01%.

Table 4.6: Search Range of Bearing Parameters and their Estimated Values

Parameters	Specified Search Range	Estimated Values
Mass of shaft	$0.01 \leq m_s \leq 2$	0.1276
Mass of pedestal	$0.01 \leq m_p \leq 2$	1.6705
Mass of resonator	$0.01 \leq m_r \leq 2$	0.7122
Stiffness of shaft	$1 \times 10^6 \leq k_s \leq 1 \times 10^8$	8.981×10^7
Stiffness of pedestal	$1 \times 10^6 \leq k_p \leq 1 \times 10^8$	1.459×10^7
Stiffness of resonator	$1 \times 10^8 \leq k_r \leq 1 \times 10^{10}$	4.234×10^9
Load distribution factor	$1 \times 10^{11} \leq k_b \leq 1 \times 10^{12}$	6.2168×10^{11}
Damping of shaft	$2 \times 10^3 \leq c_s \leq 1 \times 10^4$	4.4728×10^3
Damping of pedestal	$2 \times 10^3 \leq c_p \leq 1 \times 10^4$	6.4385×10^3
Damping of resonator	$2 \times 10^3 \leq c_r \leq 1 \times 10^4$	5.3820×10^7
Clearance	$1 \times 10^{-7} \leq c \leq 1 \times 10^{-5}$	8.291×10^{-7}
Slippage	$0.008 \leq slip \leq 0.02$	0.0182

Figure 4.10 shows a comparison between simulated signals of the model with estimated parameters and experimental signal of outer race fault is shown. The characteristic frequency spectra of the simulated signal is 46.39 Hz while that of the experimental data is 45.95 Hz. This reveals the accuracy of the bearing model that has parameters estimated through PSO because it compares closely to the experimental characteristic frequency and the theoretical ball pass frequency of inner race. The accuracy stands at 99.39%. These results show that the estimated parameters produced a model with more accurate characteristic frequencies Mbagaya et al., 2021 The accuracy of the bearing model improves from 97.88% to 99.01% for outer race faults and from 98.35% to 99.39% for inner race faults. This shows that the bearing parameters were accurately identified using PSO giving rise to more accurate models that represent the bearing system.

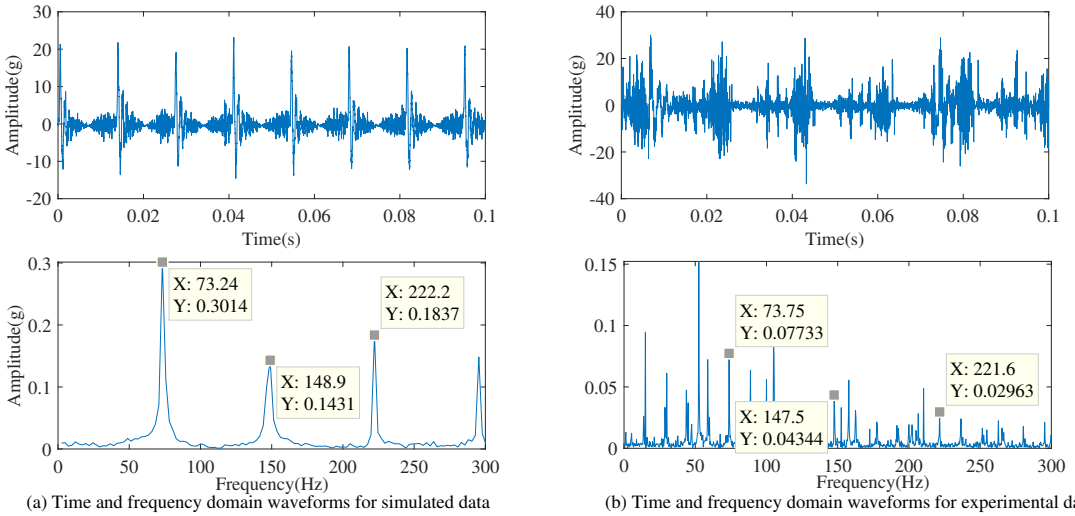

(a) Time and frequency domain waveforms for simulated data

(b) Time and frequency domain waveforms for experimental data

Figure 4.9: Vibration response of inner race fault of simulated signal (a) vs experimental data (b)

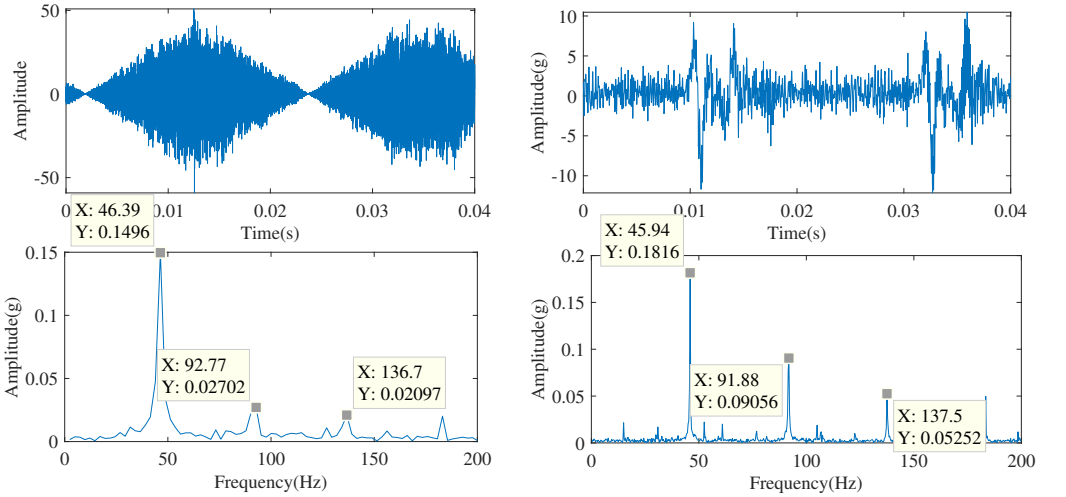

(a)Time and frequency domain waveforms for simulated data

(b) Time and frequency domain waveforms for experimental data

Figure 4.10: Vibration response of outer race fault of simulated signal (a) vs experimental data (b)

4.4 Effect of Varying Defect Depth and Width

An evaluation of how an increase in defect depth and width impacts the fault detection of a rolling element bearing system is done and the effect of varying the fault severity is studied. Initially, the bearing fault depth in the outer race and inner race is varied from 0.9 mm, 1 mm, and 3 mm while the defect width is held constant at 0.001 rad. The choice of values for defect depth and width was informed by the experimental results that used the same values. Table 4.7 shows readings of the peak amplitudes of the bearing characteristic frequency as the defect depth increases for both a fault in the outer race and inner race.

Table 4.7: Varying bearing defect depth

Defect Depth(mm)	Defect Location	Amplitude
0.9	OR	0.08809
1	OR	0.1087
3	OR	0.1482
0.9	IR	0.04803
1	IR	0.04801
3	IR	0.05743

The results show that as the defect depth increases, the peak amplitude of the bearing characteristic frequency also increases for both faults in the outer race and inner race respectively. The increase in the peak amplitudes may be due to the higher impact forces as the bearing falls into the defect and since the accelerations are closely associated with impact forces, the larger the impact force, the higher the accelerations and thus translating to higher peak amplitudes of characteristic frequency. Sample vibration results with a defect depth of 3 mm in the outer race is shown in Figure 4.11.

The bearing width is also varied from 0.001 rad to 0.003 rad while the depth of 2mm is held constant. Table 4.8 shows the results of a change in amplitude with change

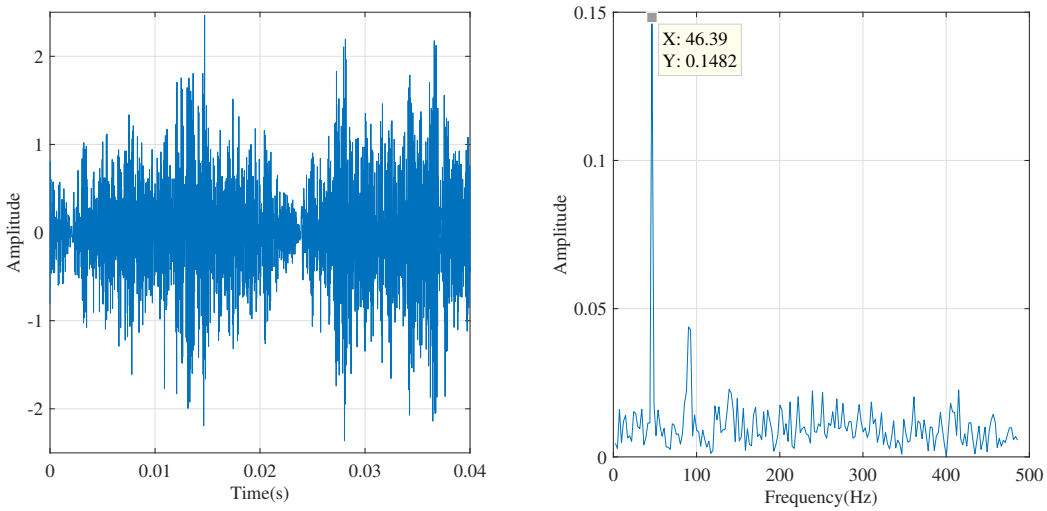

Figure 4.11: Simulation of outer race fault with a defect depth of 3mm

in bearing defect depth. For the outer race defect, the peak frequency amplitude increases initially then decreases as defect width increases. For the inner race defect, the same phenomena is observed. The peak amplitude of the characteristic defect frequency initially increases then decreases on increasing the defect width. It was therefore not possible to find a correlation between the defect width and the peak amplitudes of the characteristic frequencies because of the variations observed.

Table 4.8: Varying bearing defect width

Defect Width(radians)	Defect Location	Amplitude
0.001	OR	0.06692
0.002	OR	0.1502
0.003	OR	0.1482
0.001	IR	0.4184
0.002	IR	0.05677
0.003	IR	0.03838

4.5 Simulation of the Bearing Degradation Process

Sample results of simulation of bearing degradation in normal stage and in failure stage is shown in Figure 4.12 and Figure 4.13 respectively. In Figure 4.12 shows obvious impacts with a period of $\tau = 0.2117s$ which corresponds to the fault characteristic frequency. Severe fault vibration signal usually has obvious periodical impulses due to the defects in the raceway or rolling elements. The whole degradation process of the bearing was simulated, with signals repeated 50 times with increasing fault severity.

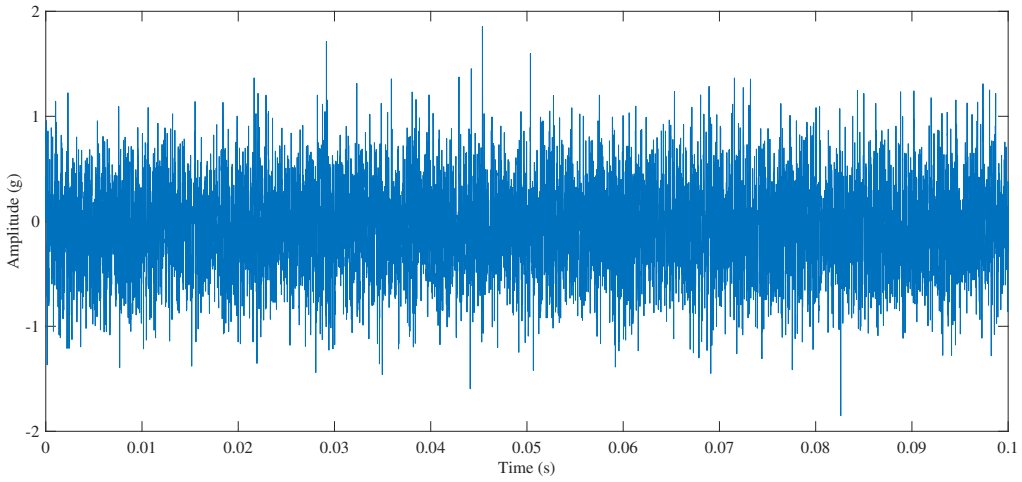

Figure 4.12: Simulation of bearing in normal stage

4.6 Feature Extraction

Statistical features such as RMS, kurtosis, skewness and crest factor were derived from the simulated vibration signals on the basis that they are commonly used parameters for condition monitoring of bearing. Figure 4.14 shows the results of the statistical features with increasing defect severity.

It is seen that the RMS of the vibration signal increases during the degradation

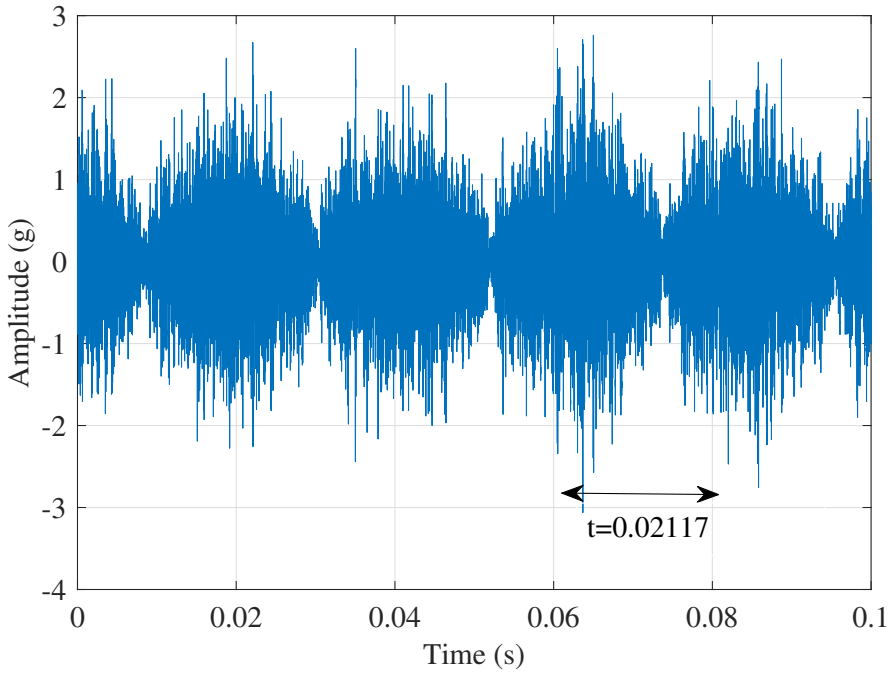

Figure 4.13: Simulation of bearing in failure stage

process. For a healthy bearing, the RMS value usually remains stationary (Lim & Mba, 2015). However, as soon as the bearing develops a fault, the RMS value begins to increase. Figure 4.14 (a) shows how RMS changes as bearing fault increases. The figure shows a monotonically increasing degradation trend throughout the bearing lifetime. Depending upon the rate of defect propagation and damage growth, the RMS value can exhibit both linear and highly non-linear trends.

Figure 4.14 (b) reveals that the kurtosis index is sensitive to the incipient faults of the bearing but not informative for the development of the fault. In literature, a healthy bearing is known to have a kurtosis value of 3. Any value greater than 3 indicates degradation of the bearing as witnessed at t=500 min. Therefore, t=500 min indicates the initial time of the degradation process. To evaluate the performance of the HI's, comparisons based on monotonicity (Mon), correlation (Corr), and robustness (Rob) was carried out and the results are as shown in Table 4.9. The table shows a comparison of health indicators based on monotonicty,

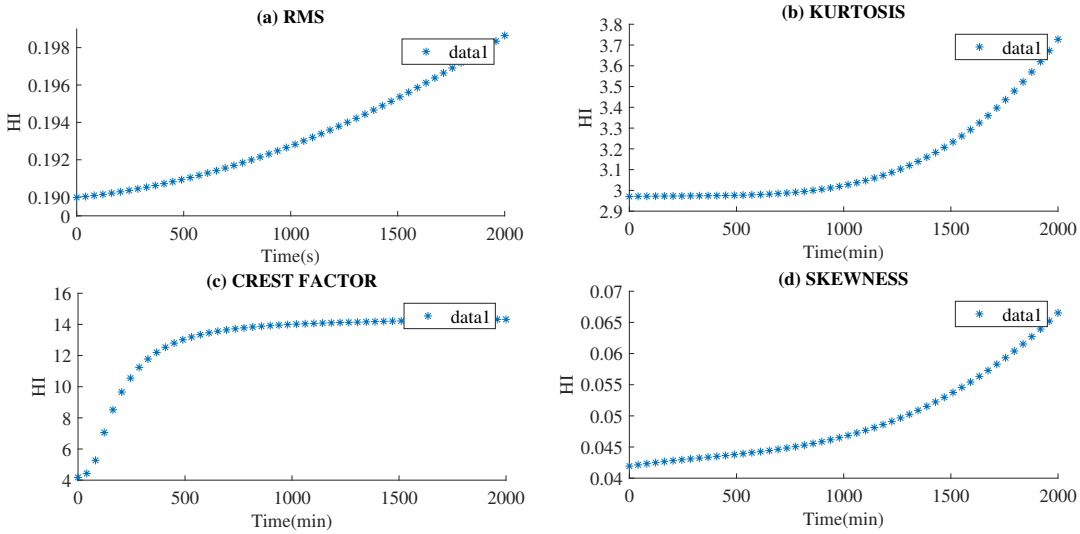

Figure 4.14: Extracted Features

robustness and trendability.

Table 4.9: Comparison of health indicators based on Monotonicity, Robustness and Trendability

Metrics	RMS	Kurtosis	Skewness	Crest Factor
Mon	0.7587	0.7436	0.7229	0.5290
Rob	0.8437	0.8958	0.8368	0.7339
Tre	0.8694	0.8439	0.8489	0.5494

The results reveal that all Mon, Rob, and Tre of RMS is higher than that of Kurtosis, Skewness and Crest Factor thus demonstrating that RMS will yield a better HI.

4.7 RUL estimation with RMS as HI

The RMS values were input into the Paris model for prediction of remaining useful life. Figure 4.15 shows the results from parameter estimation process. The model parameters m_k and C_k, and the damage state a_k were estimated using the measured

RMS data. Firstly, the true RMS data is generated using $m_{true} = 3.8$ and $C_{true} = 1.5 \times 10^{-10}$. The measured RMS data were then generated by multiplying noise, which is lognormally distributed with standard deviation of $0.001/a_k$.

In the beginning of the prediction process, it can be seen that all the parameters are not correctly estimated. However, all these parameters converge to the actual values when adequate RMS values are used in the parameter estimation. Once the model parameters were identified after updating process, the future behavior of degradation could be easily predicted by propagating the model to the future time, i.e., substituting the identified parameters to the degradation model with future time and loading

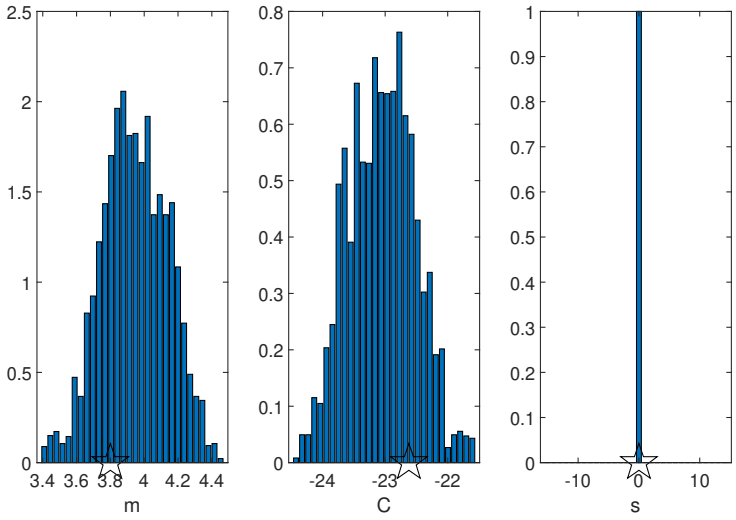

Figure 4.15: Parameter estimation using Bayesian method with Markov Chain Monte Carlo simulation

Figure 4.16 shows the prediction of degradation trend of RMS using Paris Model. In this diagram, the black line is the Paris degradation Model, the black dots are the RMS data, the red dash is the median, the red dot is the 90% prediction interval, and the green line is the failure threshold. It can be seen that the RMS tracking results of the Paris model almost coincide with the real RMS values. This shows

that the Paris model has succeeded in restraining random errors of the stochastic process due to the smooth degradation process.

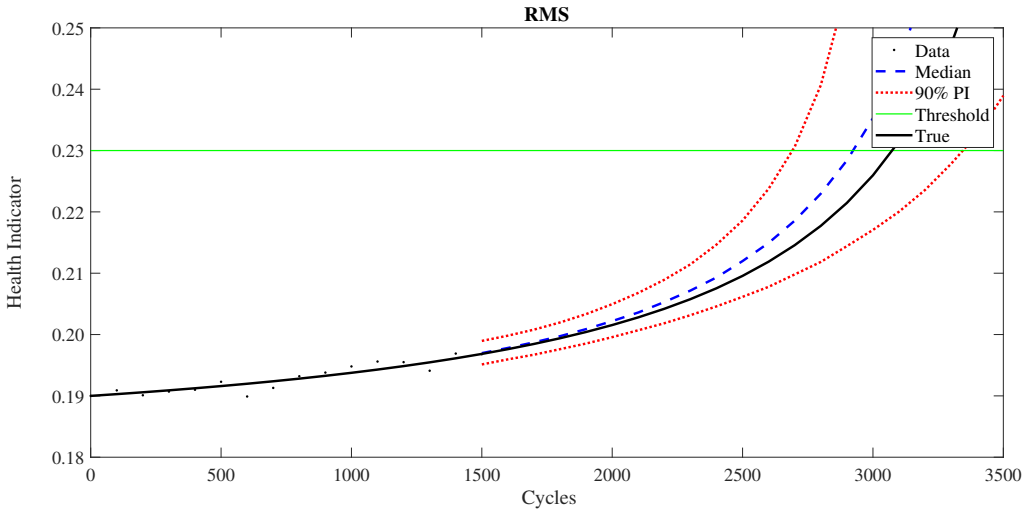

Figure 4.16: Prediction of degradation trend using Paris Model

In order to calculate the RUL, the degradation state was propagated until it reached the threshold. The threshold was determined to be 0.23 due to the fact that beyond this point, increase in fault severity did not cause any change in RMS value. The RUL distribution was obtained for each inspection interval with the newly updated HI and the parameters. Figure 4.17 shows the RUL prediction results in the degradation stage.

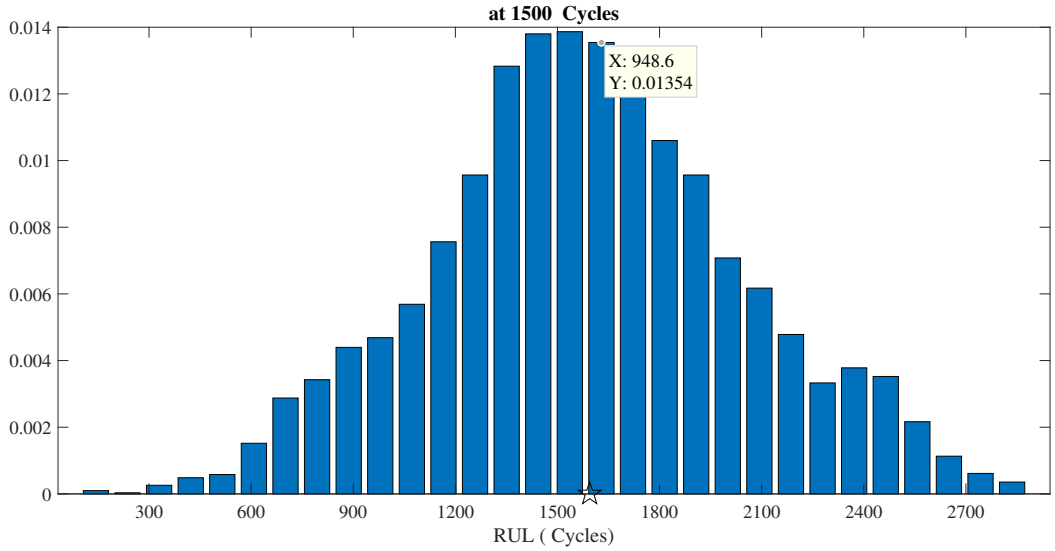

Figure 4.17: RUL prediction results

From the results, the percentiles of RUL at 1500 cycles is given as follows: 5th is 405.86, 50th(median) is 1598.45 and 95th is 2689.93. These results indicate that the developed model was successful in estimating the remaining useful life of bearings and can be investigated further in bearing prognostics.

4.8 Summary

In this section, the bearing degradation model was developed using Paris model and remaining useful life of bearing was determined.Validation of the model was done using 2 sets of publicly available data from Case Western University and University of Paderborn. Results showed that there was an overall improved accuracy in diagnosing bearing faults with the model having parameters estimated using PSO algorithm. The similarity between the simulated and measured signals shows the robustness of the developed model and its suitability for testing new diagnostic and prognostic methods (Sawalhi, 2007). The results from the feature extraction of bearing data simulated with increasing severity showed statistical trends that were monotonically increasing albeit at different rates. From the assesment of

the statistical features, it was revealed that RMS featured best in monotonicity, robustness, and trendability and hence, it's selection as the health indicator for the degradation model. The degradation model developed using Paris Model was then used to estimate the remaining useful life.

CHAPTER FIVE

CONCLUSIONS AND RECOMMENDATIONS

5.1 Summary

Mathematical models are important in the analysis, design, and fault diagnosis and prognosis of rotor-bearing systems. However, due to the complex structure and other factors, it is impossible to establish an accurate physical model. Thus, in this thesis, a model-based method of the nonlinear, rotor-bearing system based on Particle Swarm Optimisation (PSO) algorithm was proposed. The simulated bearing model was accurate in diagnosing bearing faults. With PSO, the accuracy averaged at 99.67% and 99.2% for bearing faults of Case Western Reserve University and University of Paderborn datasets, respectively. Validation with experimental results indicate that the parameter estimation with PSO can accurately recreate the underlying nonlinearity of rotorbearing system. Furthermore, the model was used to estimate the remaining useful life through the use of Bayesian method with Markov Chain Monte Carlo method. Root mean square (RMS) was used as the health indicator after a quantitative assessment of the health indicators showed that it ranked better in monotonicity, trendability and robustnesss. This method enriches the nonlinear, rotor-bearing modeling theory and provides a reliable model for dynamic analysis, design, and fault condition monitoring of the rotor-bearing system, which is of practical significance.

5.2 Conclusion

Following the successful completion of this study, it was concluded that:

1. The bearing developed in SIMULINK had an accuracy of 98.5% and 98.32% for outer and inner race faults from CWRU dataset, and an accuracy of 98.35% and 97.88% for outer and inner race faults from University of Paderborn dataset. This implies that the bearing model developed was accurate in diagnosing bearing faults

2. After estimation of parameters using PSO algorithm, the accuracy averaged at 99.67% and 99.2% for bearing faults of Case Western Reserve University and University of Paderborn datasets. The improvement in accuracy points to the effectiveness of PSO in parameter estimation.

3. The comparison of performance metrics such as monotonicity, robustness and trendability revealed that RMS was the more suitable health indicator compared to kurtosis, skewness and crest factor.

4. The remaining useful life of the bearing was found to be 1598 cycles. The prediction results and evaluation indexes demonstrated the effectiveness and superiority of use of Paris Model for bearing degradation with RMS as health indicator.

5.3 Recommendations

This research can be used in industries to improve reliability prediction in the design of safety-critical systems, reduce life cycle costs due to condition-based maintenance practices and can lead to benefits in production due to better process quality control and integrated maintenance development by OEMs (Lee et al., 2014).

The following recommendations are made for further investigation in this area of study:

- Apply the proposed bearing diagnostics technique to diagnostics of bearings with multiple faults
- Comparison of PSO with other algorithms in estimating the bearing dynamic parameters
- Use of other health indicators such as kurtosis to estimate the remaining useful life of bearings
- Implementation of the remaining useful life estimation in an actual system to show the effectiveness of the proposed approach

REFERENCES

Ahmad, W., Khan, S. A., & Kim, J. (2018). A hybrid prognostics technique for rolling element bearings using adaptive predictive models. *IEEE Transactions on Industrial Electronics*, *65*(2), 1577–1584. https://doi.org/10.1109/TIE.2017.2733487

Alam, M. (2016, March). Particle swarm optimization: Algorithm and its codes in matlab. https://doi.org/10.13140/RG.2.1.4985.3206

Alam, M., Das, B., & Pant, V. (2015). A comparative study of metaheuristic optimization approaches for directional overcurrent relays coordination. *Electric Power Systems Research*, *128*, 39–52. https://doi.org/10.1016/j.epsr.2015.06.018

Alewine, K., & Chen, W. (2012). A review of electrical winding failures in wind turbine generators. *IEEE Electrical Insulation Magazine*, *28*(4), 8–13.

Alfi, A. (2011). Pso with adaptive mutation and inertia weight and its application in parameter estimation of dynamic systems. *Acta Automatica Sinica*, *37*. https://doi.org/10.1016/S1874-1029(11)60205-X

Alonge, F., DIppolito, F., & Raimondi, F. (2001). Least squares and genetic algorithms for parameter identification of induction motors. *Control Engineering Practice*, *9*(6), 647–657. https://doi.org/https://doi.org/10.1016/S0967-0661(01)00024-7

Antoniadou, I, Manson, G, Staszewski, W., Barszcz, T, & Worden, K. (2015). A time–frequency analysis approach for condition monitoring of a wind turbine gearbox under varying load conditions. *Mechanical Systems and Signal Processing*, *64*, 188–216.

Bian, L., & Gebraeel, N. (2014). Stochastic modeling and real-time prognostics for multi-component systems with degradation rate interactions. *IIE Transactions*, *46*(5), 470–482.

Boashash, B. (2015). *Time-frequency signal analysis and processing: A comprehensive reference*. Academic Press.

Bonnett, A. H., & Yung, C. (2008). Increased efficiency versus increased reliability. *IEEE Industry Applications Magazine*, *14*(1), 29–36.

Case western reserve university bearing data center [Date when last accessed: 2020-06-29]. (n.d.). https://csegroups.case.edu/bearingdatacenter/pages/download-data-file

Chinnam, R. B., & Baruah, P. Autonomous diagnostics and prognostics through competitive learning driven hmm-based clustering. In: *Proceedings of the international joint conference on neural networks, 2003. 4*. IEEE. 2003, 2466–2471.

Coble, J. (2021). Merging data sources to predict remaining useful lifean automated method to identify prognostic parameters.

Cocconcelli, M., Zimroz, R., Rubini, R., & Bartelmus, W. Stft based approach for ball bearing fault detection in a varying speed motor. In: *Condition monitoring of machinery in non-stationary operations*. Springer, 2012, pp. 41–50.

Daigle, M. J., & Goebel, K. (2011). A model-based prognostics approach applied to pneumatic valves. *International Journal of Prognostics and Health Management*, *2*(2), 84–99.

Deng, W., Yao, R., Zhao, H., Yang, X., & Li, G. (2019). A novel intelligent diagnosis method using optimal ls-svm with improved pso algorithm. *Soft Computing*, *23*, 2445–2462.

Deshpande, L. G. (2014). Simulation of vibrations caused by faults in bearings and gears. http://handle.unsw.edu.au/1959.4/53647

Djeddi, M., Granjon, P., & Leprettre, B. Bearing fault diagnosis in induction machine based on current analysis using high-resolution technique. In: *2007*

ieee international symposium on diagnostics for electric machines, power electronics and drives. IEEE. 2007, 23–28.

Dong, M., & He, D. (2007). A segmental hidden semi-markov model (hsmm)-based diagnostics and prognostics framework and methodology. *Mechanical Systems and Signal Processing*, *21*(5), 2248–2266.

Eberhart, R., & Kennedy, J. A new optimizer using particle swarm theory. In: *Mhs'95. proceedings of the sixth international symposium on micro machine and human science*. Ieee. 1995, 39–43.

Elwany, A. H., & Gebraeel, N. Z. (2008). Sensor-driven prognostic models for equipment replacement and spare parts inventory. *IIe Transactions*, *40*(7), 629–639.

Feng, P., Xiao-Ting, L., Qian, Z., Wei-Xing, L., & Qi, G. (2013). Analysis of standard particle swarm optimization algorithm based on markov chain. *Acta Automatica Sinica*, *39*(4), 381–389.

Feng, Z., & Liang, M. (2014). Fault diagnosis of wind turbine planetary gearbox under nonstationary conditions via adaptive optimal kernel time–frequency analysis. *Renewable Energy*, *66*, 468–477.

Gao, Z., Cecati, C., & Ding, S. X. (2015). A survey of fault diagnosis and fault-tolerant techniquespart i: Fault diagnosis with model-based and signal-based approaches. *IEEE Transactions on Industrial Electronics*, *62*(6), 3757–3767.

Gašperin, M., Juričić, Đ., Boškoski, P., & Vižintin, J. (2011). Model-based prognostics of gear health using stochastic dynamical models. *Mechanical Systems and Signal Processing*, *25*(2), 537–548.

Ge, X., Luo, Z., Ma, Y., Liu, H., & Zhu, Y. (2019). A novel data-driven model based parameter estimation of nonlinear systems. *Journal of Sound and Vibration*, *453*, 188 –200. https://doi.org/https://doi.org/10.1016/j.jsv.2019.04.024

Gebraeel, N., Lawley, M., Liu, R., & Parmeshwaran, V. (2004). Residual life predictions from vibration-based degradation signals: A neural network approach. *IEEE Transactions on Industrial Electronics*, *51*(3), 694–700.

Gebraeel, N. Z., & Lawley, M. A. (2008). A neural network degradation model for computing and updating residual life distributions. *IEEE Transactions on Automation Science and Engineering*, *5*(1), 154–163.

Guan, Y., Liang, M., & Necsulescu, D.-S. (2017). A velocity synchrosqueezing transform for fault diagnosis of planetary gearboxes under nonstationary conditions. *Proceedings of the Institution of Mechanical Engineers, Part C: Journal of Mechanical Engineering Science*, *231*(15), 2868–2884.

Han, F., Guo, X., & Gao, H. (2013). Bearing parameter identification of rotor-bearing system based on kriging surrogate model and evolutionary algorithm. *Journal of Sound and Vibration*, *332*(11), 2659–2671.

Harris, T., & Yu, W. K. (1999). Lundberg-palmgren fatigue theory: Considerations of failure stress and stressed volume.

Harris, T. A. (2001). *Rolling bearing analysis*. John Wiley; sons.

Heng, A., Zhang, S., Tan, A. C., & Mathew, J. (2009). Rotating machinery prognostics: State of the art, challenges and opportunities. *Mechanical Systems and Signal processing*, *23*(3), 724–739.

Hiyama, T. et al. Development of artificial neural network based fault diagnosis of induction motor dearing. In: *2008 ieee 2nd international power and energy conference*. IEEE. 2008, 1387–1392.

Ioannides, E., Harris, T., & Ragen, M. (1990). Endurance of aircraft gas turbine mainshaft ball bearings-analysis using improved fatigue life theory: Part 1application to a long-life bearing.

Isermann, R. (2011). *Fault-diagnosis applications: Model-based condition monitoring: Actuators, drives, machinery, plants, sensors, and fault-tolerant systems*. Springer Science & Business Media.

Jardine, A. K., Lin, D., & Banjevic, D. (2006). A review on machinery diagnostics and prognostics implementing condition-based maintenance. *Mechanical Systems and Signal processing*, *20*(7), 1483–1510.

Javed, K., Gouriveau, R., Zerhouni, N., & Nectoux, P. (2015). Enabling health monitoring approach based on vibration data for accurate prognostics. *IEEE Transactions on Industrial Electronics*, *62*(1), 647–656. https://doi.org/10.1109/TIE.2014.2327917

Jiang, K., Zhu, C., Chen, L., & Qiao, X. (2015). Multi-dof rotor model based measurement of stiffness and damping for active magnetic bearing using multi-frequency excitation. *Mechanical Systems and Signal Processing*, *60*, 358–374.

Jin, Q., Wang, K., Zhang, J., & Cao, L. (2014). A novel hybrid pso identification method simultaneously estimate model parameter and the structure. *Applied Mathematics & Information Sciences*, *8*(4), 1789.

Kacprzynski, G., Sarlashkar, A, Roemer, M., Hess, A, & Hardman, B. (2004). Predicting remaining life by fusing the physics of failure modeling with diagnostics. *JOM*, *56*(3), 29–35.

Kim, N.-H., An, D., & Choi, J.-H. (2017). Prognostics and health management of engineering systems. *Switzerland: Springer International Publishing*.

Kim, Y.-H., Yang, B.-S., & Tan, A. C. (2007). Bearing parameter identification of rotor–bearing system using clustering-based hybrid evolutionary algorithm. *Structural and Multidisciplinary Optimization*, *33*(6), 493–506.

Lee, J., Wu, F., Zhao, W., Ghaffari, M., Liao, L., & Siegel, D. (2014). Prognostics and health management design for rotary machinery systemsreviews, methodology and applications. *Mechanical Systems and Signal processing*, *42*(1-2), 314–334.

Lei, Y., Li, N., Guo, L., Li, N., Yan, T., & Lin, J. (2018). Machinery health prognostics: A systematic review from data acquisition to rul prediction.

Mechanical Systems and Signal Processing, *104*, 799–834. https://doi.org/https://doi.org/10.1016/j.ymssp.2017.11.016

Li, C. J., & Lee, H. (2005). Gear fatigue crack prognosis using embedded model, gear dynamic model and fracture mechanics. *Mechanical Systems and Signal processing*, *19*(4), 836–846.

Li, N., Lei, Y., Lin, J., & Ding, S. X. (2015). An improved exponential model for predicting remaining useful life of rolling element bearings. *IEEE Transactions on Industrial Electronics*, *62*(12), 7762–7773. https://doi.org/10.1109/TIE.2015.2455055

Liao, H., & Tian, Z. (2013). A framework for predicting the remaining useful life of a single unit under time-varying operating conditions. *IIE Transactions*, *45*(9), 964–980.

Lim, C. K. R., & Mba, D. (2015). Switching kalman filter for failure prognostic. *Mechanical Systems and Signal Processing*, *52-53*, 426–435. https://doi.org/https://doi.org/10.1016/j.ymssp.2014.08.006

Lin, Q., Liu, S., Zhu, Q., Tang, C., Song, R., Chen, J., Coello, C. A. C., Wong, K.-C., & Zhang, J. (2016). Particle swarm optimization with a balanceable fitness estimation for many-objective optimization problems. *IEEE Transactions on Evolutionary Computation*, *22*(1), 32–46.

Liu, T., Chen, J., Dong, G., Xiao, W., & Zhou, X. (2013). The fault detection and diagnosis in rolling element bearings using frequency band entropy. *Proceedings of the Institution of Mechanical Engineers, Part C: Journal of Mechanical Engineering Science*, *227*(1), 87–99.

Malhi, A., Yan, R., & Gao, R. X. (2011). Prognosis of defect propagation based on recurrent neural networks. *IEEE Transactions on Instrumentation and Measurement*, *60*(3), 703–711.

Mao, W., Han, X., Liu, G., & Liu, J. (2016). Bearing dynamic parameters identification of a flexible rotor-bearing system based on transfer matrix method. *Inverse Problems in Science and Engineering*, *24*(3), 372–392.

Mbagaya, L. L, Kimotho, J. K, & Njiri, J. G. A review on prognosis of rolling element bearings operated under non-stationary conditions. In: *Sustainable research and innovation*. 2017.

Mbagaya, L. L, Kimotho, J. K, & Njiri, J. G. (2021). Parameter identification of rolling element bearing system using particle swarm optimisation algorithm: An application to fault diagnostics. *Journal of Sustainable Research in Engineering*, *6*, 87–99.

Mohamad, T. H., Nazari, F., & Nataraj, C. Model-based fault diagnostics of servo valves. In: *Annual conference of the phm society. 10*. (1). 2018.

Oppenheimer, C. H., & Loparo, K. A. Physically based diagnosis and prognosis of cracked rotor shafts. In: *Component and systems diagnostics, prognostics, and health management ii. 4733*. International Society for Optics and Photonics. 2002, 122–132.

Orchard, M. E., & Vachtsevanos, G. J. (2009). A particle-filtering approach for on-line fault diagnosis and failure prognosis. *Transactions of the Institute of Measurement and Control*, *31*(3-4), 221–246.

Orsagh, R., Brown, D., Roemer, M., Dabnev, T, & Hess, A. Prognostic health management for avionics system power supplies. In: *2005 ieee aerospace conference*. IEEE. 2005, 3585–3591.

Orsagh, R. F., Sheldon, J., & Klenke, C. J. (2003). *Prognostics/ diagnostics for gas turbine engine bearings* (Vol. 36843).

Pathak, R. S. (2009). *The wavelet transform* (Vol. 4). Springer Science & Business Media.

Peng, Y., Dong, M., & Zuo, M. J. (2010). Current status of machine prognostics in condition-based maintenance: A review. *The International Journal of Advanced Manufacturing Technology*, *50*(1-4), 297–313.

Raje, N., Sadeghi, F., Rateick, R. G., & Hoeprich, M. R. (2008). A numerical model for life scatter in rolling element bearings. *Journal of tribology*, *130*(1).

Roemer, M. J., Byington, C. S., & Sheldon, J. (2008). Advanced vibration analysis to support prognosis of rotating machinery components. *International Journal of COMADEM*, *11*(2), 2.

Samadani, M., Kwuimy, C. A., & Nataraj, C. (2014). *Fault detection and severity analysis of servo valves using recurrence quantification analysis* (tech. rep.). Villanova University Villanova United States.

Sawalhi, N. (2007). Diagnostics, prognostics and fault simulation for rolling element bearings. http://handle.unsw.edu.au/1959.4/40544

Sawalhi, N., & Randall, R. (2008). Simulating gear and bearing interactions in the presence of faults: Part i. the combined gear bearing dynamic model and the simulation of localised bearing faults. *Mechanical Systems and Signal Processing*, *22*(8), 1924–1951.

Sengupta, S., Basak, S., & II, R. (2018). Particle swarm optimization: A survey of historical and recent developments with hybridization perspectives. https://doi.org/10.3390/make1010010

Shi, Y. et al. Particle swarm optimization: Developments, applications and resources. In: *Proceedings of the 2001 congress on evolutionary computation (ieee cat. no. 01th8546). 1.* IEEE. 2001, 81–86.

Sikorska, J., Hodkiewicz, M., & Ma, L. (2011). Prognostic modelling options for remaining useful life estimation by industry. *Mechanical Systems and Signal processing*, *25*(5), 1803–1836.

Singh, S., & Tiwari, R. (2018). Model based identification of crack and bearing dynamic parameters in flexible rotor systems supported with an auxiliary active magnetic bearing. *Mechanism and Machine Theory*, *122*, 292 –307. https://doi.org/https://doi.org/10.1016/j.mechmachtheory.2018.01.006

Sinha, J. K., & Elbhbah, K. (2013). A future possibility of vibration based condition monitoring of rotating machines. *Mechanical Systems and Signal Processing*, *34*(1-2), 231–240.

Sudhakar, G., & Sekhar, A. (2011). Identification of unbalance in a rotor bearing system. *Journal of Sound and Vibration*, *330*(10), 2299–2313.

Tiwari, R, & Chakravarthy, V. (2006). Simultaneous identification of residual unbalances and bearing dynamic parameters from impulse responses of rotor–bearing systems. *Mechanical Systems and Signal Processing*, *20*(7), 1590–1614.

Tiwari, R, Lees, A., & Friswell, M. (2004). Identification of dynamic bearing parameters: A review. *Shock and Vibration Digest*, *36*(2), 99–124.

Tiwari, R., & Chougale, A. (2014). Identification of bearing dynamic parameters and unbalance states in a flexible rotor system fully levitated on active magnetic bearings. *Mechatronics*, *24*(3), 274–286.

Tobon-Mejia, D. A., Medjaher, K., Zerhouni, N., & Tripot, G. A mixture of gaussians hidden markov model for failure diagnostic and prognostic. In: *2010 ieee international conference on automation science and engineering*. IEEE. 2010, 338–343.

University of paderborn bearing data center [Date when last accessed: 2020-06-15]. (n.d.). https://mb.uni-paderborn.de/en/kat/main-research/datacenter/bearing-datacenter/data-sets-and-download/

Vachtsevanos, G, & Wang, P. Fault prognosis using dynamic wavelet neural networks. In: *2001 ieee autotestcon proceedings. ieee systems readiness technology conference.(cat. no. 01ch37237)*. IEEE. 2001, 857–870.

Wang, H., & Chen, P. (2009). Fault diagnosis method based on kurtosis wave and information divergence for rolling element bearings. *WSEAS Transactions on systems*, *8*(10), 1155–1165.

Wang, W., & Zhang, W. (2005). A model to predict the residual life of aircraft engines based upon oil analysis data. *Naval Research Logistics (NRL)*, *52*(3), 276–284.

Xia, X., Zhou, J., Xiao, J., & Xiao, H. (2016). A novel identification method of volterra series in rotor-bearing system for fault diagnosis. *Mechanical Systems and Signal Processing*, *66*, 557–567.

Yin, Q., Zhou, L., & Wang, X. (2010). Parameter identification of hysteretic model of rubber-bearing based on sequential nonlinear least-square estimation. *Earthquake engineering and engineering vibration*, *9*(3), 375–383.

Yu, W. K., & Harris, T. A. (2001). A new stress-based fatigue life model for ball bearings. *Tribology Transactions*, *44*(1), 11–18.

Zhang, B., Zhang, L., & Xu, J. (2016). Degradation feature selection for remaining useful life prediction of rolling element bearings. *Quality and Reliability Engineering International*, *32*(2), 547–554. https://doi.org/https://doi.org/10.1002/qre.1771

Zhang, S., Ma, L., Sun, Y., & Mathew, J. Asset health reliability estimation based on condition data. In: *Proceedings of the 2nd world congress on engineering asset management and the 4th international conference on condition monitoring*. Coxmoor Publishing Company. 2007, 2195–2204.

Zhang, X., Xu, R., Kwan, C., Liang, S. Y., Xie, Q., & Haynes, L. An integrated approach to bearing fault diagnostics and prognostics. In: *Proceedings of the 2005, american control conference, 2005.* IEEE. 2005, 2750–2755.

Zhang, X., Hu, N., Hu, L., Chen, L., & Cheng, Z. (2015). A bearing fault diagnosis method based on the low-dimensional compressed vibration signal. *Advances in Mechanical Engineering*, *7*(7), 1687814015593442.

Zheng, Y.-x., & Liao, Y. (2016). Parameter identification of nonlinear dynamic systems using an improved particle swarm optimization. *Optik*, *127*(19), 7865–7874.

Appendices

APPENDIX A

Bearing Model

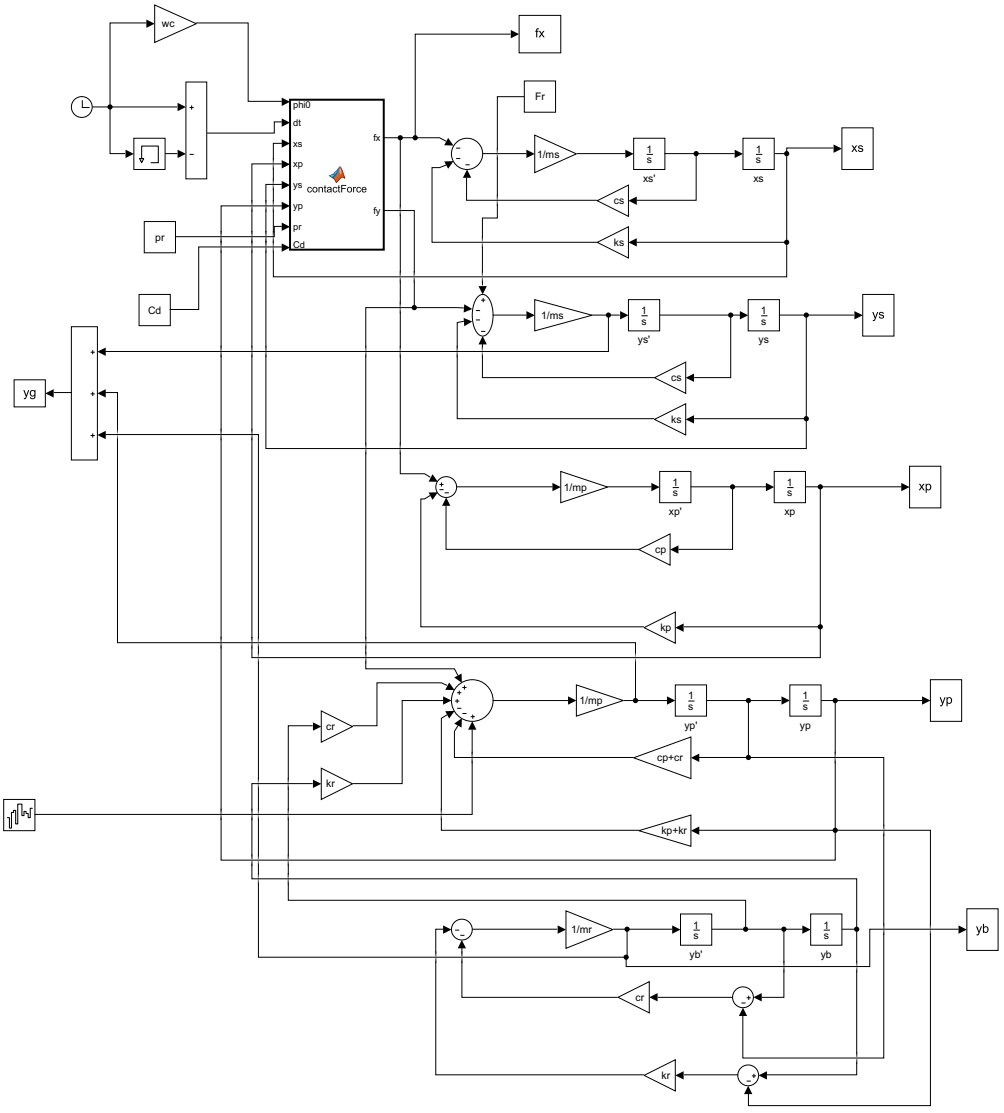

Figure A.1: Bearing Model in SIMULINK

APPENDIX B

Particle Swarm Optimisation Algorithm

```
% This class uses PSO to obtain and optimize
parameters of a state model
% automatically.
%
% INPUT:
% typ = type of optimization to conduct (elm),
(svm), (mdlFit)
classdef PSOParamSearch
    properties
        op;      % the optimum parameters
        bestcv; % the best value
        bestm;  % best members
    end
    methods
        function params =
PSOParamSearch(typ,data,inOpts,Opt)
            if nargin<4
                Opt=[];
            end

[out,Xm,maxIter,criteria,dsp]=initVar(typ,data,inOp
ts,Opt);
            Dim=size(Xm,1);
            xmin=zeros(Dim,1);
            xmax=zeros(Dim,1);
            for j=1:Dim
                xmin(j) = Xm(j,1);
                xmax(j) = Xm(j,2);
            end
            pSize = 50;         % population size p
= 25 gave good results
            % Limits on the seach space (Defining
the solution space).
            vmax = .06*(xmax - xmin);  % Limiting
maximum velocity.
            p = rand(pSize,Dim);   % uniformly
distributed values from 0 to 1
```

Figure B.1: PSO algorithm code

```
            % Converting the random values to the
relevant range between xmin and xmax
            % in every dimensiton.
            for m = 1:Dim
                p(:,m) = p(:,m)*(xmax(m) - xmin(m))
+ xmin(m);
            end
            % initializing random swarm velocity
            v = 2*( rand(pSize,Dim) - 0.6 );
            for m = 1:Dim
                v(:,m) = v(:,m)* vmax(m);
            end
            %initial pbest and gbest
            pbest = p;
            pbestVal=zeros(pSize,1);
            pbestVal(1)=fitnessFun(out,p(1,:));
            gbestVal=fitnessFun(out,p(1,:));
            gbest = p(1,:);
            for m = 2:pSize
                temp = fitnessFun(out,p(m,:));
                pbestVal(m) = temp;
                if temp < gbestVal
                    gbestVal = temp;
                    gbest = p(m,:);
                end
            end
            c_1 = 3;
            c_2 = 2;
            w_in = 0.8;
            w_f = 0.3;
            %x_store = zeros(maxIter,2);
            fit_store = zeros(maxIter,1);
            avg_fitness = zeros(maxIter,1);
            iter =1;
            while (iter <= maxIter && (gbestVal >
criteria))  % for each generation
                if dsp
```

Figure B.2: PSO algorithm code (cont..)

```
                        disp(['Iteration
#',num2str(iter),' best value =
',num2str(gbestVal)])
                end
                w = w_in + (w_f -
w_in)*iter/maxIter;
                for m = 1:pSize             % for
each particle
                    for n = 1:Dim     % for each
dimension
                        v(m,n) = w * v(m,n) + c_1 *
rand * ( pbest(m,n)-p(m,n) ) + c_2 * rand *
(gbest(n) - p(m,n));
                        if abs(v(m,n)) > vmax(n)
                            v(m,n) = v(m,n) *
vmax(n)/abs(v(m,n));
                        end
                        p(m,n) = p(m,n) + v(m,n);
                        if p(m,n) > xmax(n)
                            p(m,n) = xmax(n);
                        end
                        if p(m,n) < xmin(n)
                            p(m,n) = xmin(n);
                        end
                    end
                    temp = fitnessFun(out,p(m,:));
                    if temp  <= pbestVal(m)
                        pbestVal(m) = temp;
                        pbest(m,:) = p(m,:);
                    end
                    if temp  <= gbestVal
                        gbestVal = temp;
                        gbest = p(m,:);
                    end
                end
                % Storing the position of the first
particle.
                x_store(iter,:) = p(1,:);
```

Figure B.3: PSO algorithm code (cont..)

```
                fit_store(iter) = gbestVal;
                avg_fitness(iter) =mean(pbestVal);
                iter =iter+1;
            end
            for j=1:Dim
                params.op(j)=gbest(j);
            end
            params.bestcv=fit_store;
            params.bestm=x_store;
        end
    end
end
```

Figure B.4: PSO algorithm code (cont..)